

Primary Copy
P-6-1556

UNCLASSIFIED

Copy C-5
RM SL50G13

NACA

RESEARCH MEMORANDUM

for the

Air Materiel Command, U. S. Air Force

WIND TUNNEL INVESTIGATION OF A 0.6-SCALE MODEL OF
HUGHES MX-904 TAIL SURFACE AT SUPERSONIC SPEEDS

SEVERAL COMBINATIONS OF THE TAIL WITH EACH OF
TWO FORESHORTENED BODY SEGMENTS

By Lawrence D. Guy and D. William Conner

Langley Aeronautical Laboratory
Langley Air Force Base, Va.

CLASSIFICATION CHANGED

UNCLASSIFIED

To

By authority of *TPH #27*
7-18-62

CLASSIFICATION CHANGED

No classification or security level is assigned to this document by the author or by the National Advisory Committee for Aeronautics. It is the responsibility of the recipient to determine if it is classified and if so, to what level. It is the responsibility of the recipient to declassify or decontrol this document when it is no longer needed.

CLASSIFIED DOCUMENT

This document contains classified information affecting the National Defense of the United States within the meaning of the Espionage Act, USC 7931 and 32. Its transmission or the revelation of its contents in any manner to an unauthorized person is prohibited by law. Information so classified may be imparted only to persons in the military and naval services of the United States, appropriate civilian officials and employees of the Federal Government who have a legitimate interest therein, and to United States citizens of known loyalty and discretion who of necessity must be informed thereof.

NATIONAL ADVISORY COMMITTEE
FOR AERONAUTICS

WASHINGTON

UNCLASSIFIED

UNCLASSIFIED

NASA Technical Library



3 1176 01438 5489

NACA RM SL50G13

NATIONAL ADVISORY COMMITTEE FOR AERONAUTICS

RESEARCH MEMORANDUM

for the

Air Materiel Command, U. S. Air Force

WIND-TUNNEL INVESTIGATION OF A 0.6-SCALE MODEL OF
HUGHES MX-904 TAIL SURFACE AT SUPERSONIC SPEEDS

SEVERAL COMBINATIONS OF THE TAIL WITH EACH OF
TWO FORESHORTENED BODY SEGMENTS

By Lawrence D. Guy and D. William Conner

SUMMARY

An investigation has been made in the Langley 9- by 12-inch supersonic blowdown tunnel at Mach numbers of 1.62 and 1.96 of a partial-span body with one tail surface designed for use on the Hughes Falcon (MX-904) missile. The present paper extends the work reported in NACA RM SL50E10. Force and moment data including elevator hinge moment were obtained for the conditions of the tail in the presence of a small segment of the foreshortened body, in the presence of a semispan body and attached to a semi-span body, and for the condition of the foreshortened semispan body alone.

INTRODUCTION

At the request of the Air Materiel Command, U. S. Air Forces, an investigation has been made in the Langley 9- by 12-inch supersonic blowdown tunnel of a partial-span model of the tail surface designed for use on the Hughes Falcon (MX-904) missile. The purpose of the investigation was to determine the aerodynamic characteristics of the tail and elevator (including elevator hinge moment) and the tail loading carry-over on the fuselage. The initial series of tests at Mach numbers of 1.62 and 1.96 were reported in reference 1 for the condition of the tail attached to a segment of the foreshortened fuselage. The present paper presents data obtained at the same Mach numbers for the conditions of the tail in the presence of this body. The segment of the foreshortened body was limited in size to considerably less than a half-body

UNCLASSIFIED

in order to cover the greatest possible range of conditions without exceeding the maximum-load ratings of the balance.

To evaluate the effects of body size, data were obtained for a limited range of conditions with a foreshortened half-body. Since differences in tail loading for the two body conditions result from differences in flow fields, the investigation was extended to learn more about these flow fields by measuring the pressure distribution on a two-dimensional unswept airfoil located in the region normally occupied by the elevator on each of the two bodies. Reynolds number based on the body diameter was about 2.0×10^6 . In order to expedite publication of these data, no analysis of the results is given.

SYMBOLS

All data are referred to the wind axes.

C_L lift coefficient $\left(\frac{\text{Lift}}{qS} \right)$

C_D drag coefficient $\left(\frac{\text{Drag}}{qS} \right)$

C_m pitching-moment coefficient $\left(\frac{m}{qSd} \right)$

C_l_{gross} gross rolling-moment coefficient $\left(\frac{L}{2qSd} \right)$

C_n_{gross} gross yawing-moment coefficient $\left(\frac{N}{2qSd} \right)$

C_h elevator hinge-moment coefficient
$$\left(\frac{\text{Elevator hinge moment}}{2M_a q} \right)$$

m pitching moment of model about reference lateral axis (see figs. 1 and 2)

L rolling moment of model about reference longitudinal axis (see figs. 1 and 2)

N	yawing moment about reference vertical axis
α	angle of attack, degrees
δ	elevator deflection with respect to hinge line lying in tail chord plane, degrees
B ₁	designation of partial-span body configuration permitting measurement of loads on tail only
B ₂	designation of partial-span body configuration permitting measurement of loads on body-tail combination
B ₃	designation of half-span body configuration permitting measurement of loads on tail only
B ₄	designation of half-span body configuration permitting measurement of loads on body-tail combination
T	designation of tail surface
Δp	measured pressure minus free-stream static pressure
q	free-stream dynamic pressure
S	half cross-sectional area of complete body (5.79 sq in.)
d	diameter of complete body (3.84 in.)
M _a	moment of area of elevator aft of hinge line about hinge axis (1.34 cu in.)
M	Mach number
y	spanwise distance measured from fuselage surface

MODELS

Geometric details of the body-tail combination B₄T are shown in figure 1. Geometric details of the body-tail configurations B₁T and B₃T are presented in figure 2, and photographs of the model arrangement B₂T are shown in figure 3. The models furnished by the Hughes Aircraft Company consisted of a 0.6-scale version of one tail surface designed for the Falcon (MX-904) missile and two bodies differing in segment size.

A description of the tail-surface construction, elevator-positioning method, and strain-gage installation for measuring hinge moments is given in reference 1.

For these tests the tail surface was cantilevered from a strain-gage balance which mounts flush with the tunnel floor and rotates with the model through the angle-of-attack range. The body segments B_1 and B_3 were attached to the balance housing and were separated from the tail surface by a small gap, thus permitting loads to be measured only on the tail surface. The body segment B_4 was attached to the tail surface with a small gap between the fuselage and the tunnel floor and loads were measured on the combination. An insulated charged plate attached to the fuselage permitted an indication of model fouling. Basic tail-off tests were made for the half-body B_4 without the tail.

APPARATUS

The tests were conducted in the Langley 9- by 12-inch supersonic blowdown tunnel, which is of the nonreturn type and uses the compressed air of the Langley 19-foot pressure tunnel. The absolute stagnation pressure of the air ranged from 2 to $2\frac{1}{3}$ atmospheres. A description of this tunnel, a discussion of the results of preliminary flow calibrations of the tunnel, and a discussion of factors affecting the test results obtained are presented in reference 1.

Data-recording procedures and computing methods are outlined in reference 1.

The survey airfoil shown in figures 4 and 5 was fabricated of a tool steel and was so arranged as to permit spanwise movement with a close sliding fit through the bodies B_2 and B_4 . A brass guide in the air stream used to support the airfoil minimized deflections under load. The angle of attack of the model and survey airfoil was preset for each run, and simultaneous photographic recordings were made of orifice location, orifice pressures, and stagnation pressure.

PRECISION OF DATA

As indicated in reference 1, preliminary calibration has shown the stream to be uniform within a maximum variation of Mach number of ± 1 percent.

No tare corrections have been applied to any of the data. A discussion of interaction effects between force components measured by the balance system is given in reference 1. The estimate of maximum probable errors tabulated in reference 1 for the B_2 and B_2T configurations applies to the data from tests of the B_4 and B_4T model configurations. An estimate of the maximum probable errors in the measurements taken from the tests of the B_1T and B_3T configurations is given in the following table:

Component	As measured	Coefficient
Lift	± 1 lb	± 0.02
Drag	0.1 lb	0.002
Pitching moment	1 in.-lb	0.005
Rolling moment	2 in.-lb	0.004
Yawing moment	2 in.-lb	0.004
Hinge moment	0.1 in.-lb	0.005

Angles of attack were determined by static calibration of the balance linkage system with a correction applied for twist caused by model pitching moment. The accuracy is believed to be within $\pm 0.03^\circ$. Elevator deflection angles have been corrected for twist caused by hinge moment and are believed to be accurate to within $\pm 0.1^\circ$. The pressure coefficients $\frac{\Delta p}{q}$ obtained with the survey airfoil are believed to be accurate within ± 0.003 .

TESTS

The test techniques and the manner of calibrating the hinge-moment measuring apparatus for these tests were the same as described in reference 1. After completing the tests reported in reference 1, the elevator-positioning sector was modified to extend the upper limit of the control-deflection range to about 24° . The calibration of the hinge-moment measuring apparatus performed after completion of tests on the B_1T and B_3T configurations agreed with previous calibrations. About 0.002-inch play was noticed in the outboard pin after these tests.

For tests of the B_3T and B_4T model configurations, the center line of the fuselage was displaced from the tail-surface chord plane about 0.005 inch in order to minimize fouling difficulties at high positive angles of attack and elevator deflections. Because of construction error, the body center line for the B_4 body-alone tests was displaced 0.059 inch from the balance chord axis. Since side force was not measured, the rolling moment could not be given with respect to body axis; the data presented for B_4 alone are, therefore, slightly in error. For the B_4T configuration the axes were aligned.

Since the lowest loads were obtained at $M = 1.96$, tests of the B_4T configuration were limited to that Mach number in order to stay within the maximum permissible yawing-moment limits of the strain-gage balance. For this configuration hinge-moment data were not obtained because of malfunctioning of the strain-gage system.

During the course of each test the dynamic pressure and Reynolds number decreased about 5 percent because of the decreasing pressure of the inlet air. For the range of test conditions the values of dynamic pressure as measured in pounds per square inch were about 11.2 ± 1.0 and 10.5 ± 1.0 for $M = 1.62$ and $M = 1.96$, respectively; the corresponding values of Reynolds number were $2,100,000 \pm 200,000$ and $1,900,000 \pm 200,000$, based on the full-body diameter. (The body diameter was about equal to the mean aerodynamic chord of the tail surface.)

PRESENTATION OF DATA

The data are presented in the same manner as the data of reference 1. The basic aerodynamic data are plotted in figures 6 to 10 against elevator deflection for average constant value of angle of attack at the two test Mach numbers. Exact values of both α and δ , given in tables I to V for all test points, were considered in fairing the curves. Cross plots of these data with angle of attack as the variable are presented in figures 11 to 15. The measured B_4 body-alone data are presented in figure 15. Two-dimensional airfoil-pressure data measured in the region of the tail surface are presented in figure 16 for the B_2 and B_4 body configurations at angle-of-attack values of 5° and 10° for $M = 1.96$ and of 5° for $M = 1.62$.

It should be pointed out that lift, drag, and pitching-moment data apply to a full-span tail condition with both elevators deflected. The increments obtained in gross rolling moment and gross yawing moment caused by elevator deflection, however, apply to just one control deflected on a complete model.

Inspection of the data shows that differences in tail loadings of as much as one-third resulted when body-segment size was changed. These differences are believed to have been caused by the effects of body size and profile on the upwash, boundary layer, and local velocity field in the region of the tail. Further evidence of this is indicated by the differences in the pressure surveys made in the region of the tail as influenced by the two bodies. (See fig. 16.) It should be pointed out that in the arrangements tested the flow field in which the tail was operating would differ somewhat from that of the full-length missile-body combination and, consequently, the tail characteristics would also be expected to differ.

Langley Aeronautical Laboratory
National Advisory Committee for Aeronautics
Langley Air Force Base, Va.

Lawrence D. Guy
Aeronautical Research Scientist

D. William Conner
Aeronautical Research Scientist

Approved: *Mark R. Nichols*
for Clinton H. Dearborn
Chief of Full Scale Research Division

lc

REFERENCE

1. Conner, D. William, and Guy, Lawrence D.: Wind-Tunnel Investigation of a 0.6-Scale Model of Hughes MX-904 Tail Surface at Supersonic Speeds. Tail Attached to a Segment of the Foreshortened Body. NACA RM SL50E10, U. S. Air Force, 1950.

TABLE I.- VALUES OF ANGLES OF ATTACK AND ELEVATOR

DEFLECTION FOR DATA PRESENTED IN FIGURE 6.

(B₁T configuration) M = 1.62

Average δ , deg	-8.5	-0.5	-0.5 Check	3.5	8.0	14.0	23.0
Average α , deg							
-9.77	α						
	δ						
-7.79	α						
	δ						
-5.82	α		-5.74	-5.69	-5.81	-5.87	-6.06
	δ		.07	-.06	3.68	8.19	13.99
-3.87	α		-3.84	-3.77	-3.89	-3.97	-4.28
	δ		-.05	-.04	3.57	8.09	13.87
-1.93	α		-1.91	-1.85	-1.96	-2.26	-1.95
	δ		-.14	-.14	3.49	8.02	13.69
.03	α	0	0.01	0.07	-0.05	.10	
	δ	-8.53	-.23	-.23	3.40	7.92	
1.89	α	1.93	1.94	1.98	1.87	1.84	1.78
	δ	-8.62	-.30	-.31	3.31	7.84	13.67
3.83	α	3.85	3.85	3.90	3.78	3.75	
	δ	-8.68	-.39	-.39	3.21	7.75	
5.76	α	5.77	5.74	5.79	5.66		
	δ	-8.79	-.49	-.50	3.10		
7.64	α	7.62	7.62	7.67			
	δ	-8.94	-.63	-.64			
9.49	α	9.49					
	δ	-9.13					



TABLE II.- VALUES OF ANGLE OF ATTACK AND ELEVATOR

DEFLECTION FOR DATA PRESENTED IN FIGURE 7.

(B₁T configuration) M = 1.96

Average δ , deg	-9	0	0 Check	3.5	9	14	23.5
Average α , deg							
-9.71	α				-10.42		-9.70
	δ				8.67		23.85
-7.75	α		-8.02		-7.73	-7.80	-7.58
	δ		.13		3.82	8.50	14.27
-5.82	α		-5.80		-5.80	-5.83	-5.82
	δ		.00		3.73	8.37	14.13
-3.87	α	-3.61	-3.85	-3.86	-3.87	-3.89	-3.87
	δ	-8.64	-.10	-.09	3.62	8.29	14.07
-1.93	α	-1.93	-1.92	-1.93	-1.94	-2.10	-1.91
	δ	-8.67	-.18	-.17	3.55	8.23	14.01
0	α	-.02	0	.01	.01	.19	.02
	δ	-8.73	-.24	-.24	3.49	8.13	13.93
1.94	α	1.91	1.94	1.94	1.92	1.94	1.95
	δ	-8.82	-.31	-.31	3.43	8.07	13.87
3.87	α	3.84	3.86	3.86	3.84	3.87	3.91
	δ	-8.90	-.38	-.38	3.35	7.99	13.80
5.78	α	5.75	5.77	5.77	5.74	5.81	5.85
	δ	-9.00	-.46	-.46	3.25	7.91	13.73
7.67	α	7.64	7.68	7.68	7.65		
	δ	-9.10	-.56	-.56	3.16		
9.57	α	9.52	9.59	9.58			
	δ	-9.22	-.65	-.65			
11.42	α	11.42					
	δ	-9.34					



~~CONFIDENTIAL~~

TABLE III.- VALUES OF ANGLE OF ATTACK AND ELEVATOR

DEFLECTION FOR DATA PRESENTED IN FIGURE 8.

(B₃T configuration) M = 1.62

Average δ , deg	-14.5	-14.5 Check	-9.0	-4.0	-4.0 Check	-2.0	0.5	0.5 Check
Average α , deg								
-6.02	α							
	δ							
-4.05	α							
	δ							
-1.97	α				-1.87	-1.85	-1.95	-1.96
	δ				-3.83	-3.83	-2.04	-.26
0.00	α		.43	.03	.04	.01	.02	.02
	δ		-8.46	-3.93	-3.93	-2.15	-.38	-.37
1.88	α		2.03	2.00	2.02	2.01	1.98	1.98
	δ		-8.54	-4.02	-4.02	-2.25	-.50	-.49
3.97	α	4.19	4.18	3.98	3.96	3.98	3.99	3.97
	δ	-14.23	-14.28	-8.66	-4.13	-4.13	-2.37	-.62
5.91	α	6.10	6.69	5.91	5.92	5.93	5.88	
	δ	-14.45	-14.47	-8.83	-4.29	-4.30	-2.54	
7.90	α	7.98	8.01	7.79				
	δ	-14.64	-14.67	-9.01				
9.91	α		9.91					
	δ		-14.83					

~~CONFIDENTIAL~~

TABLE III.- VALUES OF ANGLE OF ATTACK AND ELEVATOR
DEFLECTION FOR DATA PRESENTED IN FIGURE 8 - Concluded

Average δ , deg	1.5	3.0	5.0	8.0	8.0 Check	13.5	22.5	22.5 Check
Average α , deg								
-6.02	α δ				-6.02 8.13	-5.99 8.12	-6.06 13.72	
-4.05	α δ	-4.13 1.65	-3.97 3.45	-3.99 5.30		-4.03 7.98	-4.06 13.55	-4.07 22.66
-1.97	α δ	-1.98 1.51	-1.99 3.32	-2.01 5.19	-2.05 7.89	-2.03 7.89	-2.10 13.44	-4.11 22.67
0.00	α δ	.01 1.41	-.01 3.22	-.05 5.10	-.05 7.81	-.04 7.80	-.09 13.29	
1.88	α δ	1.99 1.30	1.95 3.11	1.95 4.98	1.93 7.69	1.93 7.69		
3.97	α δ	3.97 1.19	3.95 3.00					



TABLE IV.- VALUES OF ANGLE OF ATTACK AND ELEVATOR
DEFLECTION FOR DATA PRESENTED IN FIGURE 9.

(B₃T configuration) M = 1.96

Average δ , deg	-15	-15 Check	-9	-4	-2.5	-5	1.5
Average α , deg							
-8.02 α							
-8.02 δ							
-6.02 α							
-6.02 δ							
-4.00 α							
-4.00 δ							
-2.00 α			-2.02	-1.99	-1.99	-1.98	-1.99
-2.00 δ			-8.68	-3.97	-2.14	-.30	1.56
-0.01 α				-.01	0	0	0
-0.01 δ				-8.76	-4.10	-2.27	-.42
1.98 α	1.96		1.96	1.99	1.99	1.99	1.97
1.98 δ	-14.57		-8.88	-4.21	-2.38	-.55	1.31
3.96 α	3.92	3.95	3.94	4.17	3.96	3.95	3.98
3.96 δ	-14.66	-14.68	-8.99	-4.28	-2.51	-.67	1.19
5.92 α	5.89	5.89	5.91	5.92	5.95	5.92	5.93
5.92 δ	-14.76	-14.76	-9.14	-4.47	-2.65	-.82	1.06
7.86 α	7.84	7.83	7.86	7.89	7.90		
7.86 δ	-14.91	-14.89	-9.39	-4.63	-2.80		
9.83 α	9.83	9.82	9.83				
9.83 δ	-15.09	-15.09	-9.46				
11.81 α	11.83	11.79					
11.81 δ	-15.24	-15.24					



TABLE IV.- VALUES OF ANGLE OF ATTACK AND ELEVATOR
DEFLECTION FOR DATA PRESENTED IN FIGURE 9 - Concluded

Average δ , deg	4	5	8	8 Check	14	23	23 Check
Average α , deg							
-8.02	α δ				-8.02 14.17		
-6.02	α δ	-6.02 5.65	-6.00 8.38	-6.02 8.39	-6.00 14.04	-6.04 23.28	-6.02 23.27
-4.00	α δ	-3.99 3.55	-3.99 5.49	-4.00 8.24	-4.00 8.25	-4.02 13.91	-4.03 23.16
-2.00	α δ	-1.95 3.43	-1.99 5.36	-2.01 8.12	-1.99 8.11	-2.02 13.79	-2.03 23.02
-0.01	α δ	-.02 3.31	-.02 5.24	-.02 8.01	0 8.02	-.02 13.67	-.08 22.79
1.98	α δ	1.97 3.20	1.99 5.14	1.99 7.90	1.99 7.91	1.97 13.55	1.97 22.84
3.96	α δ	3.95 3.08	3.97 5.02	3.99 7.78	4.00 7.79		
5.92	α δ	5.96 2.94	5.95 4.86				



~~CONFIDENTIAL~~

NACA RM SL50G13

TABLE V.- VALUES OF ANGLE OF ATTACK AND ELEVATOR

DEFLECTION FOR DATA PRESENTED IN FIGURE 10.

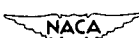
(B₄T configuration) M = 1.96

Average δ , deg		-15	-15 Check	-9.5	-6	-4	-2	0	0 Check
Average α , deg									
-4.18	α								
	δ								
-2.09	α			-1.78	-2.10	-2.00	-2.08	-2.09	-2.08
	δ			-9.24	-6.04	-4.12	-2.14	-.19	-.19
0	α	.02	.02	.03	.05	.02	.03	.01	-.01
	δ	-14.92	-14.92	-9.26	-6.06	-4.15	-2.16	-.23	-.23
2.09	α	2.10	2.10	2.13	2.04	2.12	2.13	2.09	2.08
	δ	-14.95	-14.95	-9.29	-6.09	-4.18	-2.17	-.24	-.24
4.17	α	4.18	4.17	4.18	4.13	4.20	4.20	4.17	4.17
	δ	-14.98	-14.98	-9.31	-6.12	-4.20	-2.20	-.27	-.27
6.25	α	6.25	6.24	6.25	6.21	6.28	6.28	6.20	6.23
	δ	-15.00	-15.00	-9.34	-6.15	-4.22	-2.24	-.29	-.29
8.32	α	8.33	8.31	8.34	8.28				
	δ	-15.04	-15.04	-9.37	-6.16				



TABLE V.- VALUES OF ANGLE OF ATTACK AND ELEVATOR
DEFLECTION FOR DATA PRESENTED IN FIGURE 10 - Concluded

Average δ , deg	2	3.5	3.5 Check	5.5	8.5	14.5	14.5
Average α , deg							
-4.18	α			-4.02	-4.17	-4.20	-4.18
	δ			3.74	5.67	8.66	14.55
-2.09	α	-2.11	-2.09	-2.08	-2.10	-2.07	-2.12
	δ	2.04	3.73	3.71	5.66	8.66	14.53
0	α	-.01	0	0	0	-.02	-.04
	δ	2.02	3.69	3.69	5.64	8.62	14.51
2.09	α	2.08	2.09	2.10	2.09	2.09	2.05
	δ	2.00	3.67	3.68	5.60	8.60	14.50
4.17	α	4.17	4.15	4.15	4.15	4.13	
	δ	1.97	3.64	3.64	5.58	8.58	
6.25	α	6.21		6.20			
	δ	1.94		3.62			
8.32	α						
	δ						



32171

NACA RM SL50G13

CONFIDENTIAL

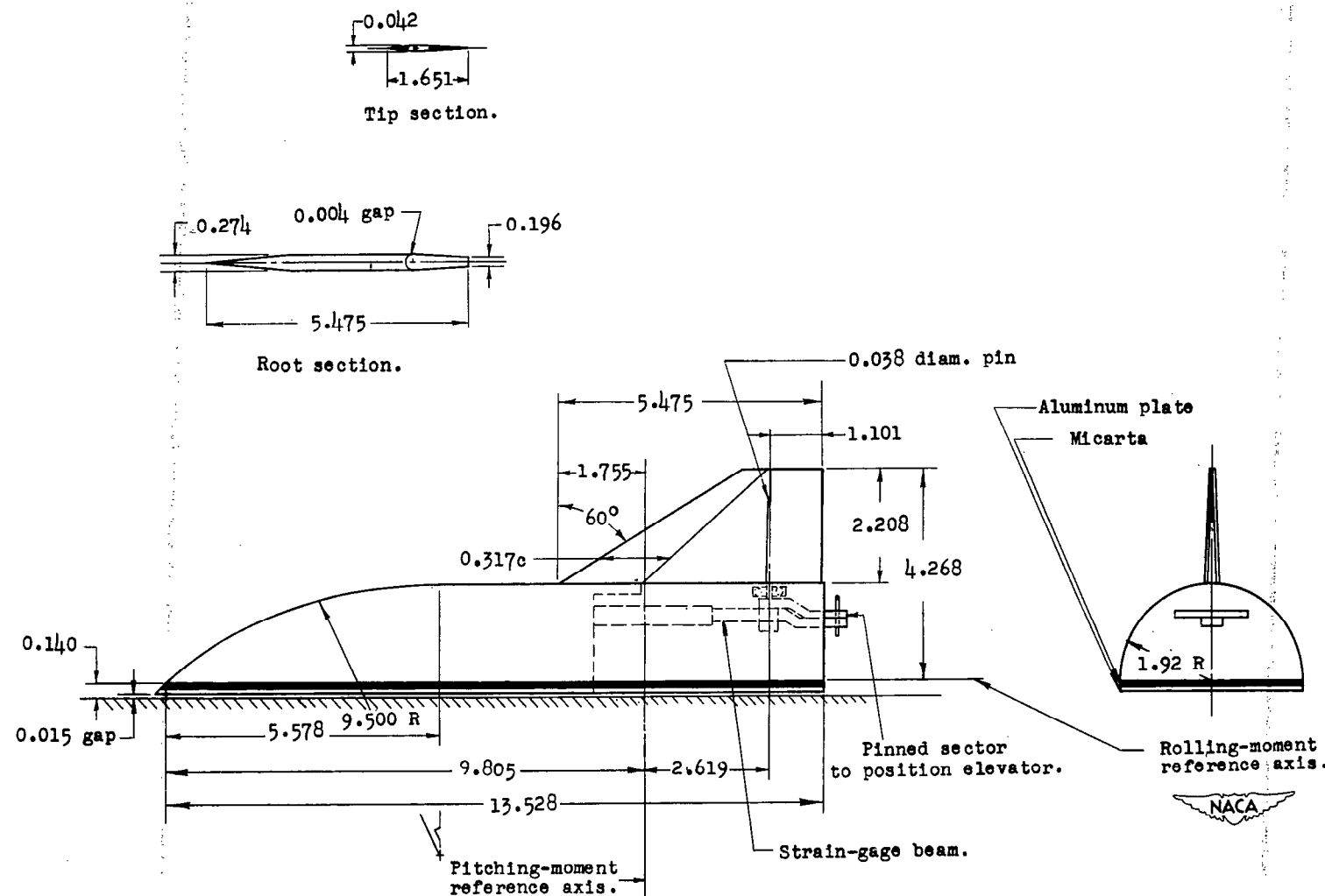
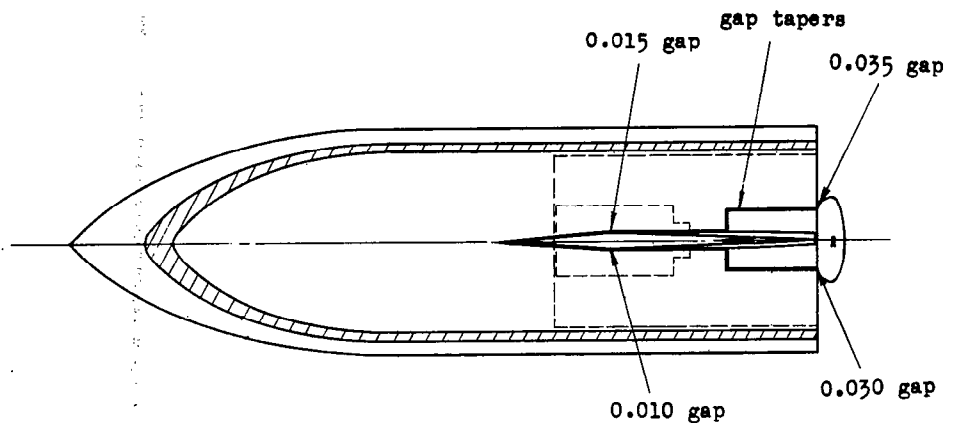


Figure 1.- Details of a 0.6-scale model of Falcon (MX-904) tail surface attached to body segment B₄. All dimensions are in inches.

3217 2

NACA RM SL50G13

CONFIDENTIAL



Body segment B_1 is formed from body segment B_3 shown by detaching body sector below parting line.

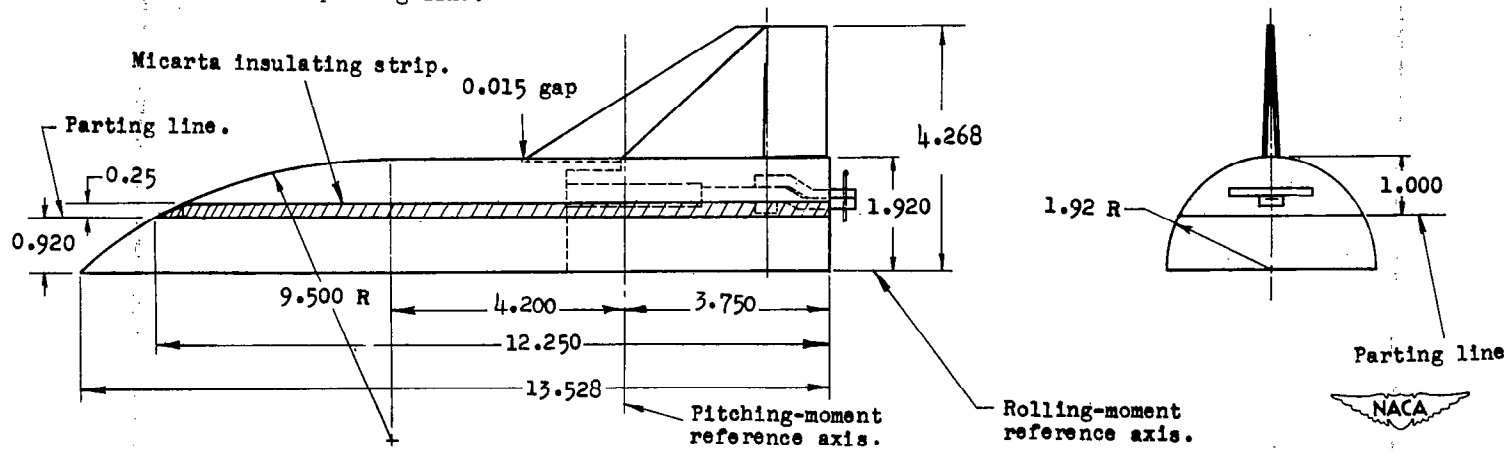


Figure 2.- Details of 0.6-scale model of Falcon (MX-904) tail surface in the presence of body configurations B_1 and B_3 . All dimensions are in inches.

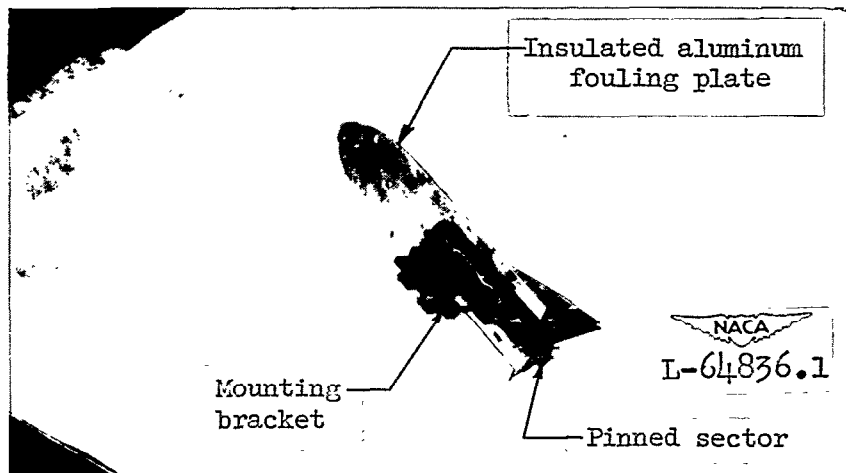
P
R
O
T

NACA RM SL50G13

P
R
O
T



(a) Model mounted for testing in Langley 9- by 12-inch blowdown tunnel with nozzle blocks removed.



(b) Details of underside of model.

Figure 3.- Photographs of 0.6-scale partial-span model of Falcon (MX-904) missile (B_2T combination).

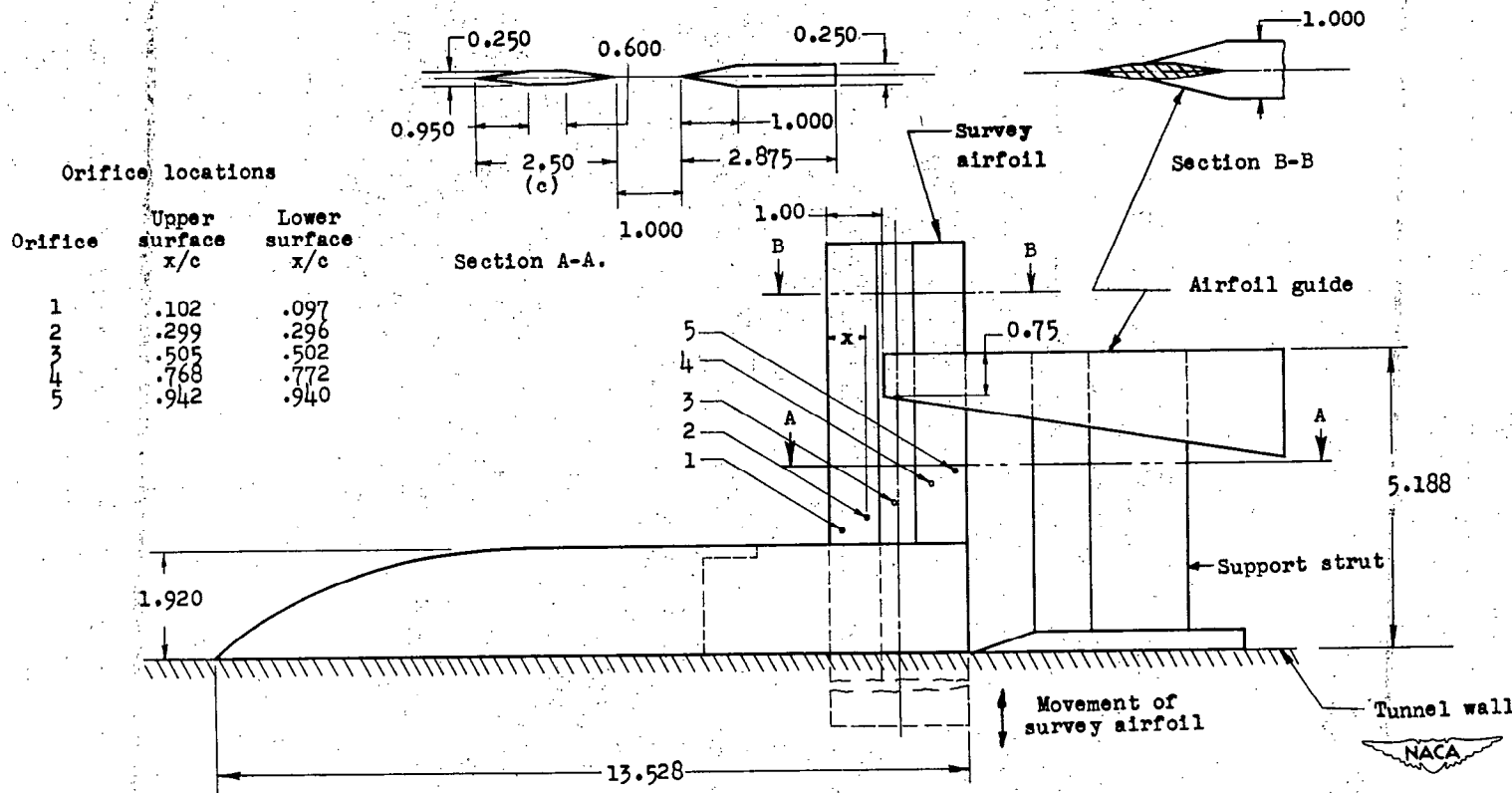


Figure 4.- Details of survey airfoil and body configuration B₄. All dimensions are in inches.

32175

NACA RM SL50G13

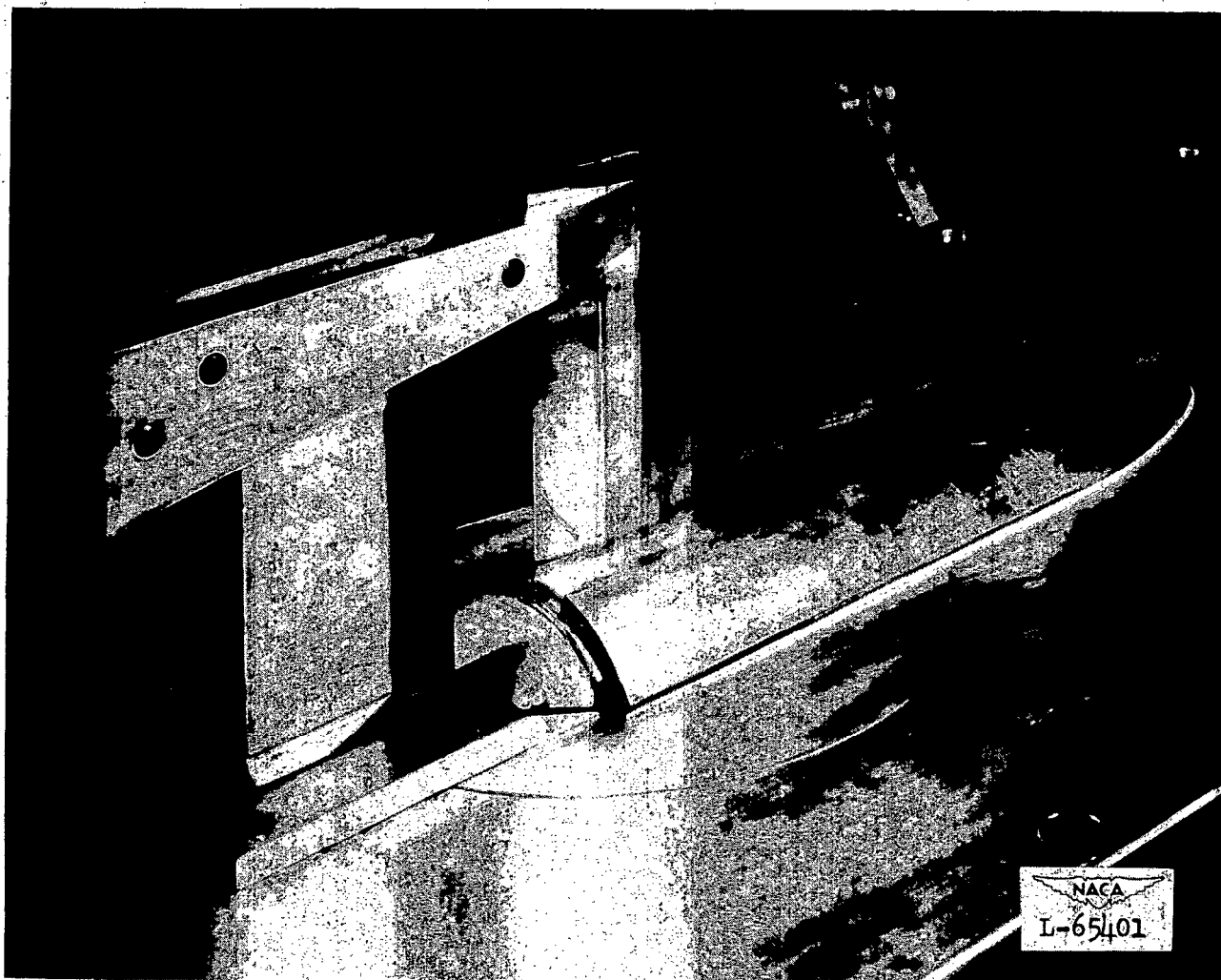
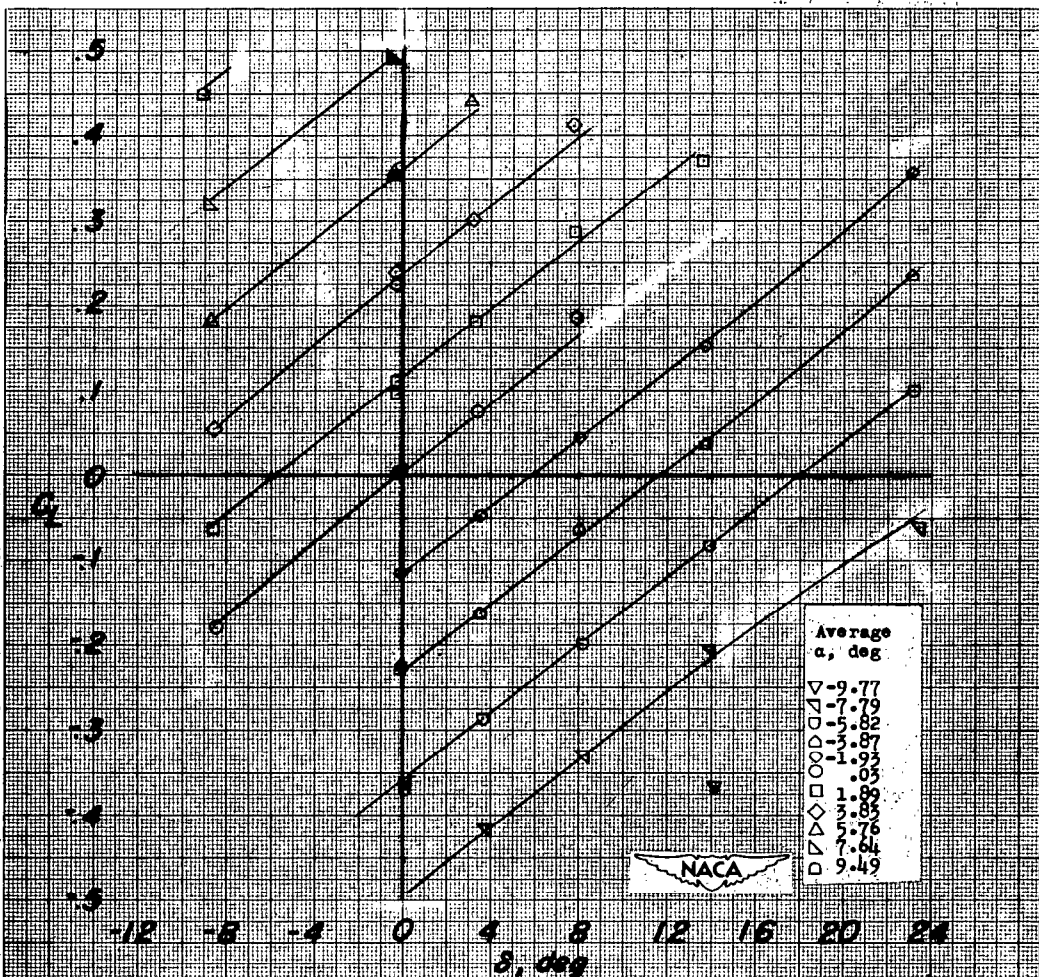
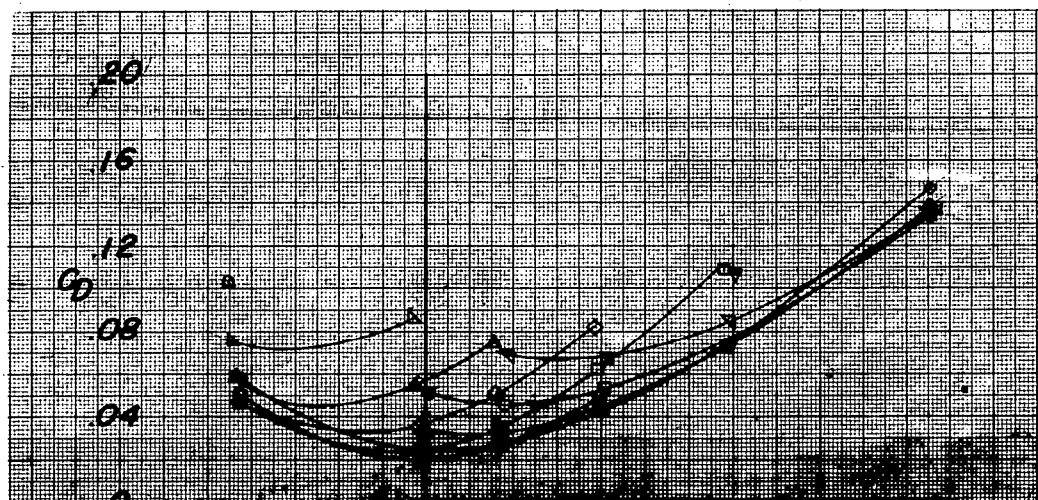


Figure 5.- Survey airfoil mounted in combination with fuselage B₂.

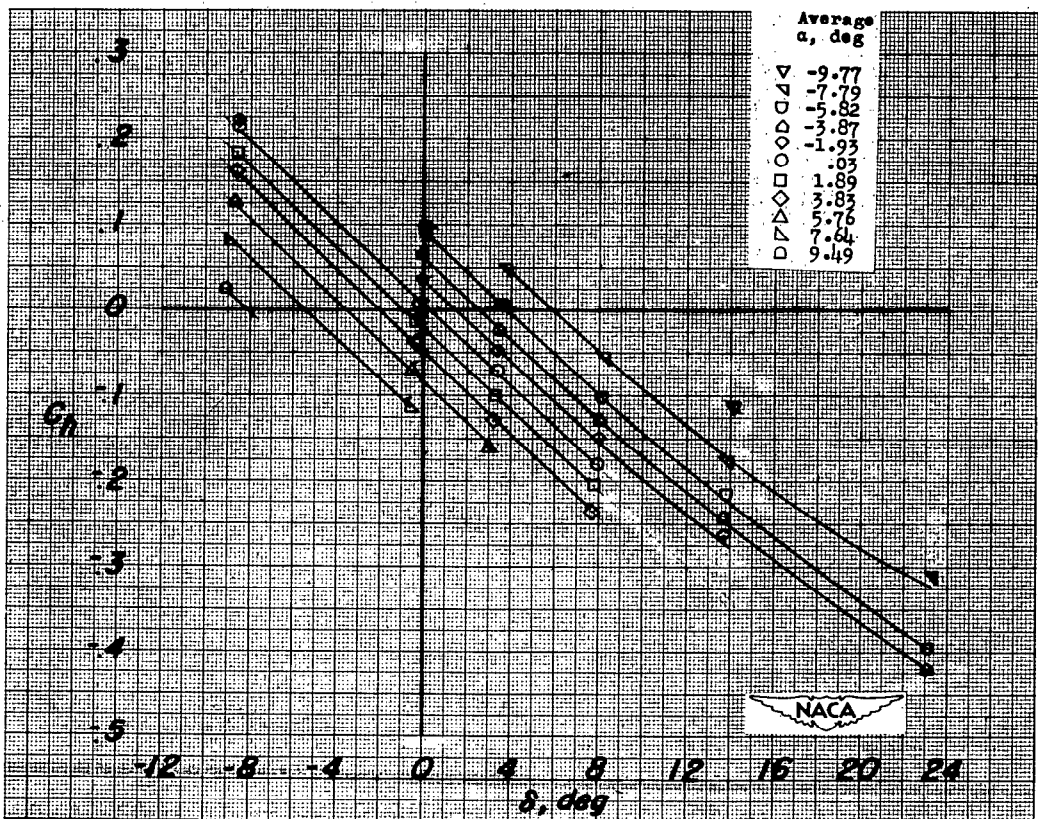


(a) Lift.

Figure 6.- Variation of aerodynamic characteristics with elevator deflection of 0.6-scale model of Falcon (MX-904) tail surface in the presence of partial-span body (B_1T); $M = 1.62$. (Flagged symbols denote check tests.)

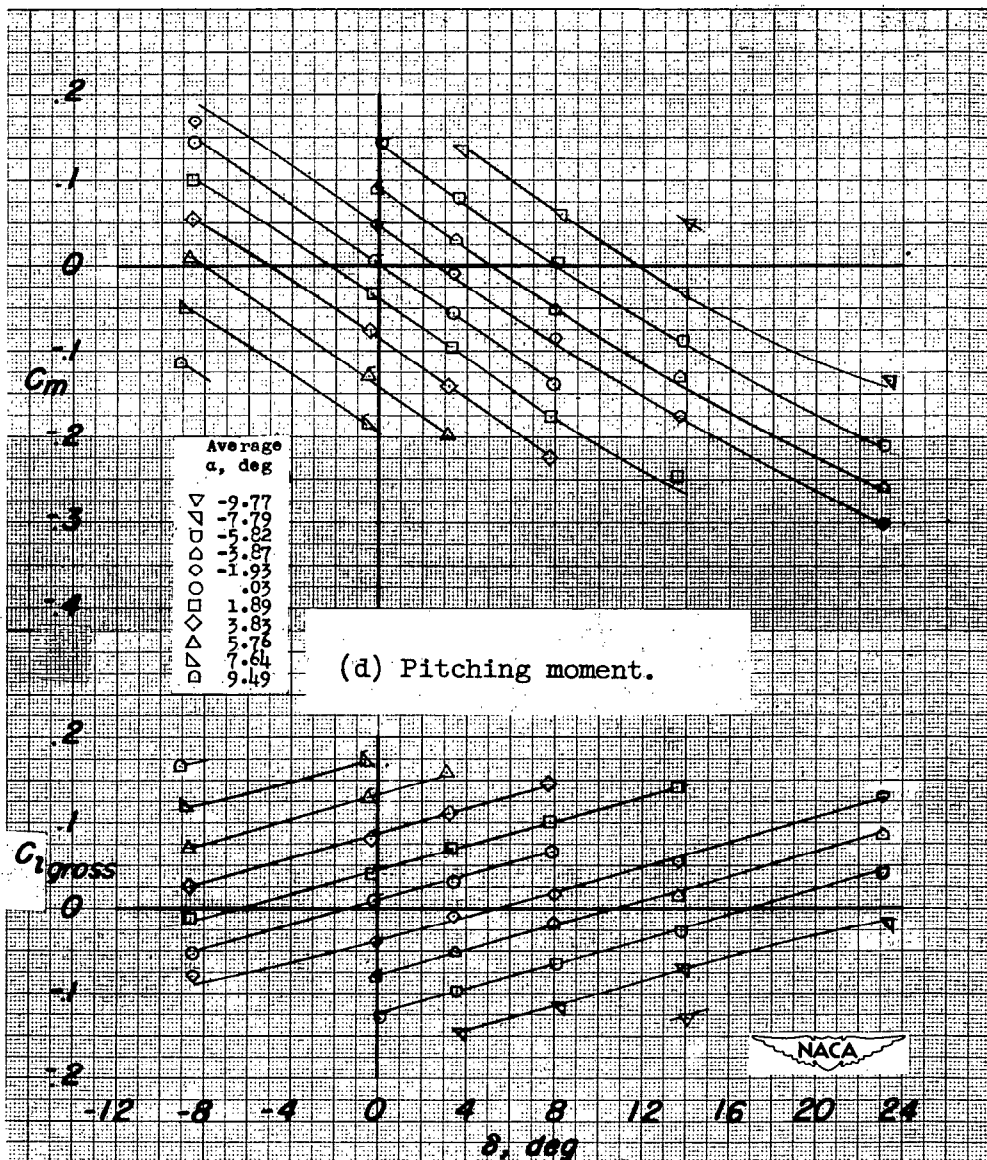


(b) Drag.



(c) Elevator hinge moment.

Figure 6.- Continued.

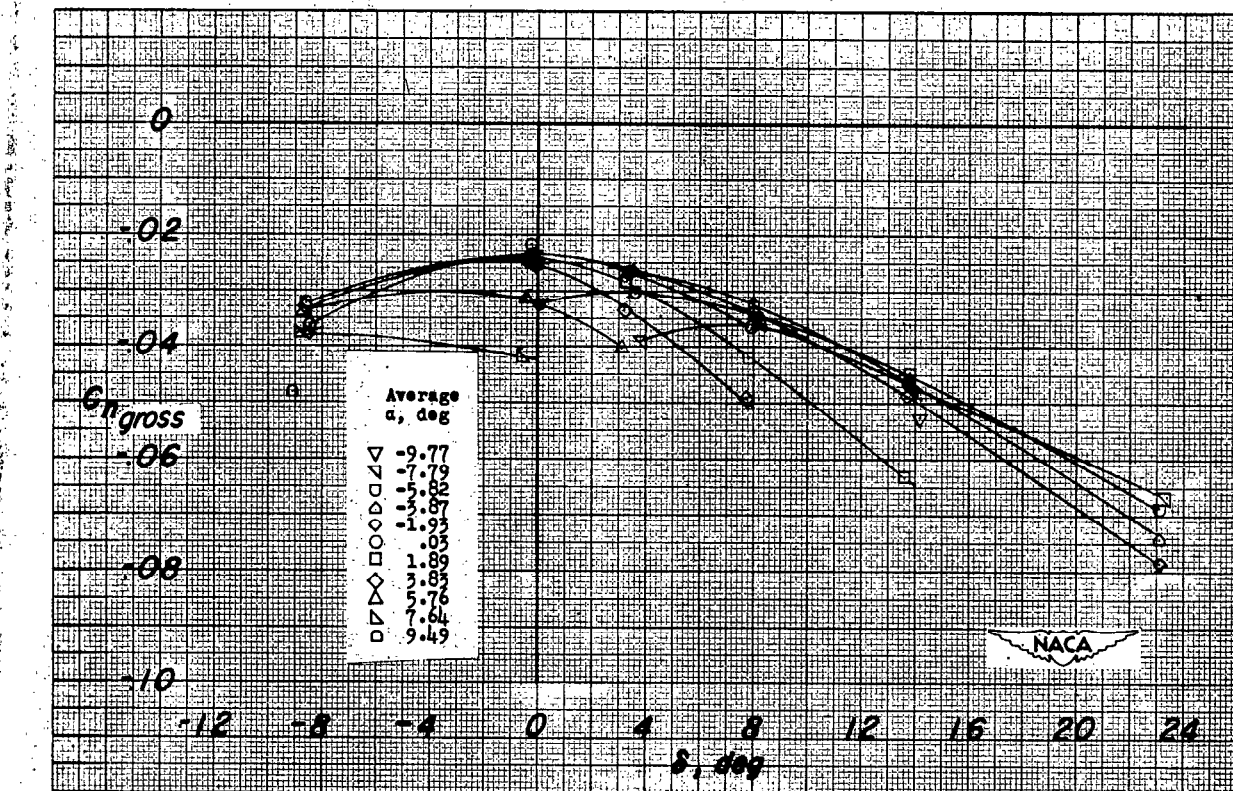


(e) Rolling moment.

Figure 6.- Continued.

3217 6
NACA RM 5150G13

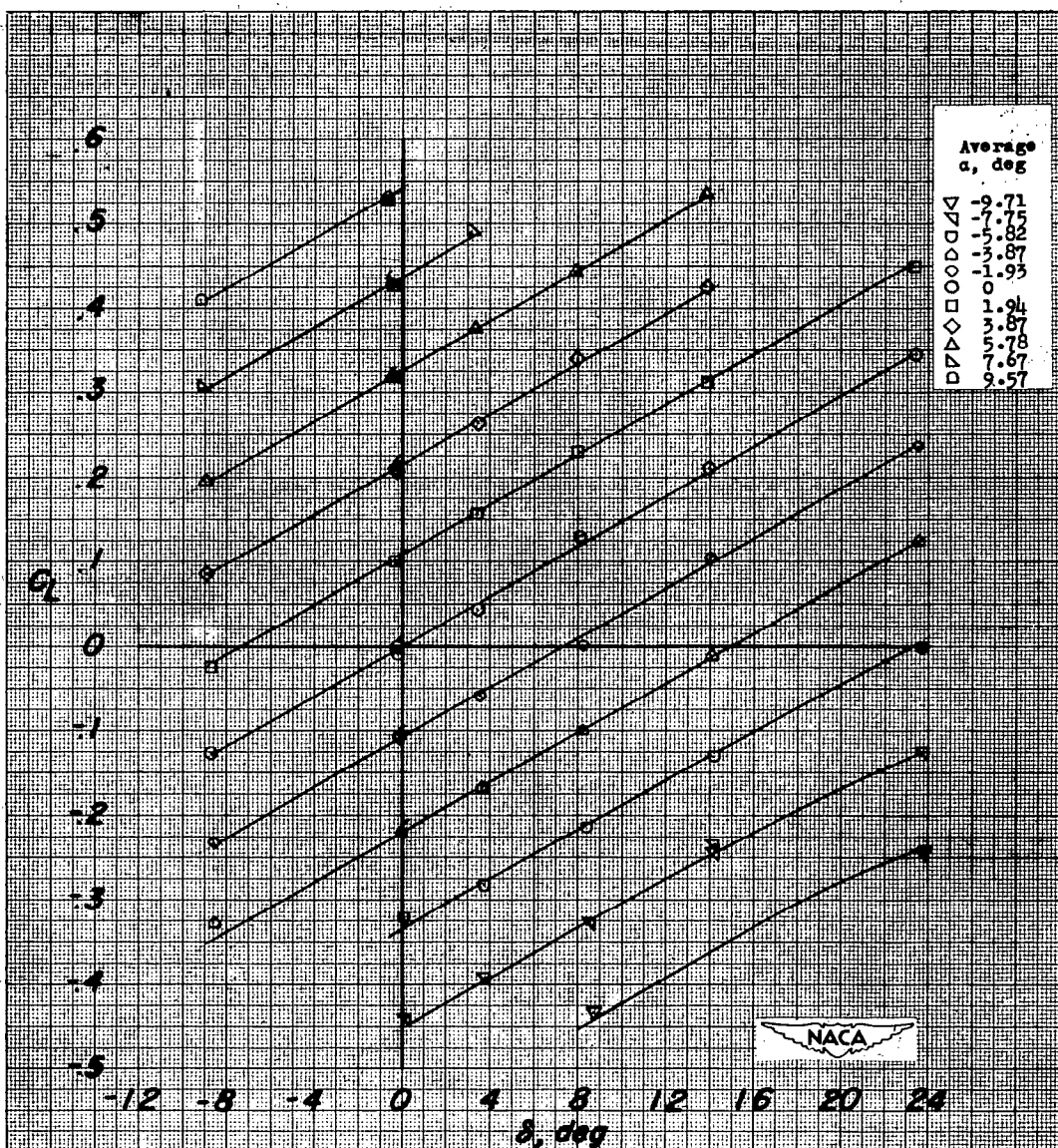
CONFIDENTIAL



(f) Yawing moment.

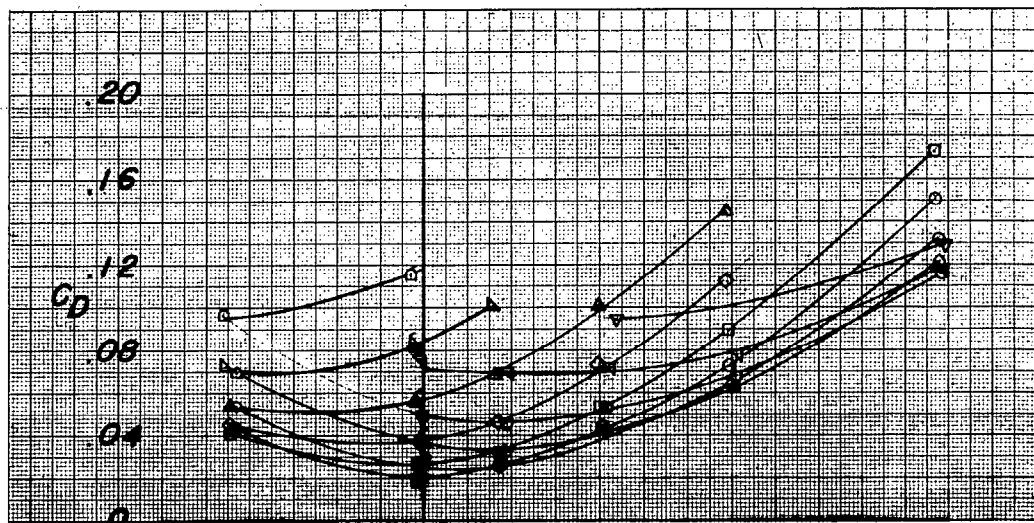
Figure 6.- Concluded.

CONFIDENTIAL

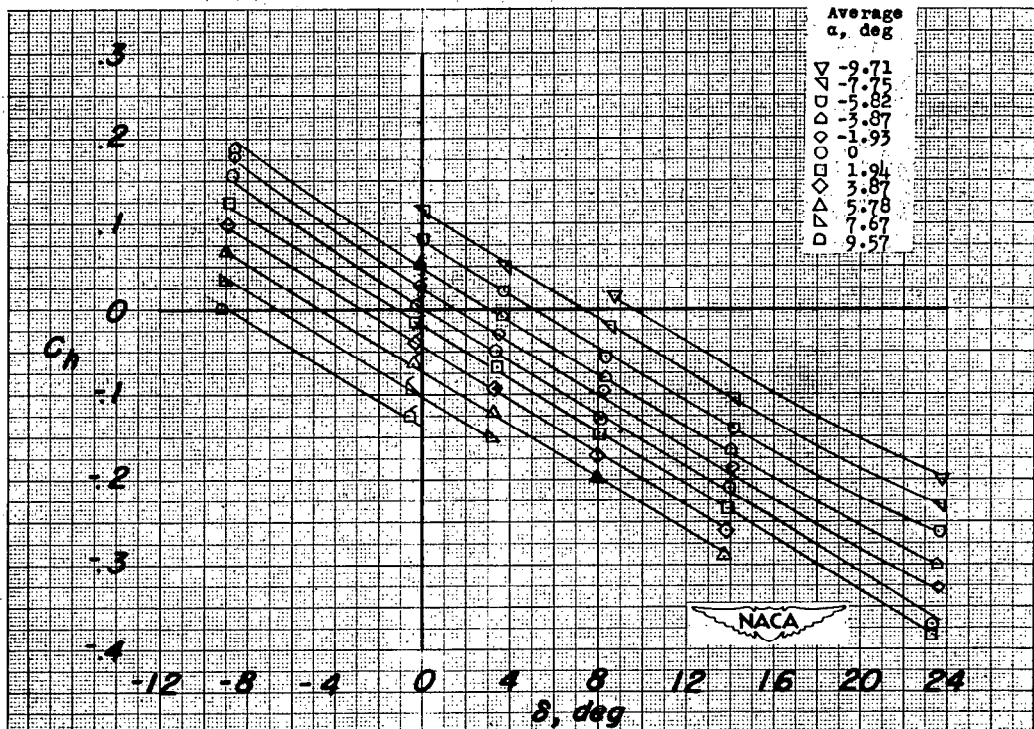


(a) Lift.

Figure 7.- Variation of aerodynamic characteristics with elevator deflection of 0.6-scale model of Falcon (MX-904) tail surface in the presence of partial-span body (B_{1T}); M = 1.96. (Flagged symbols denote check tests.)

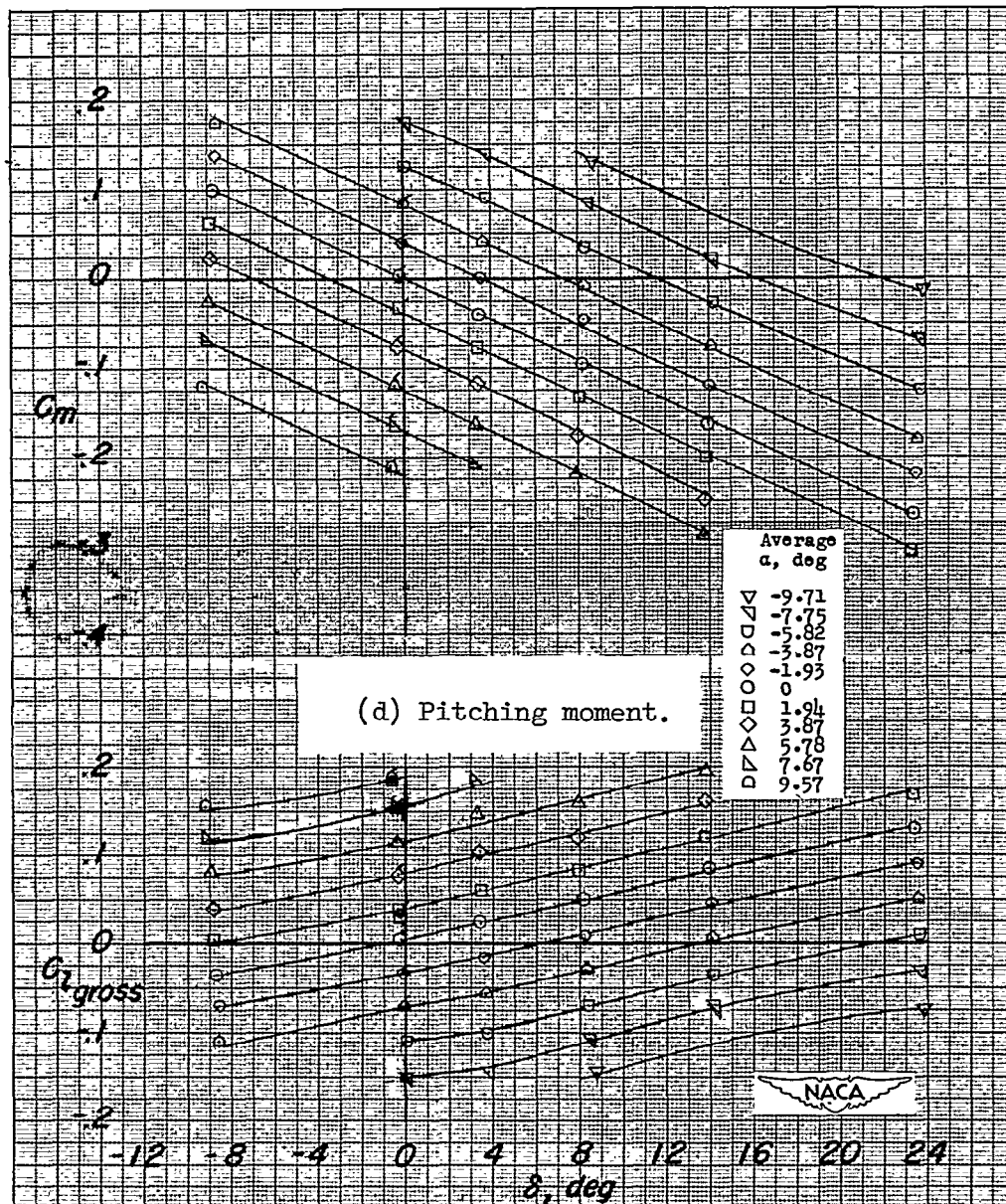


(b) Drag.



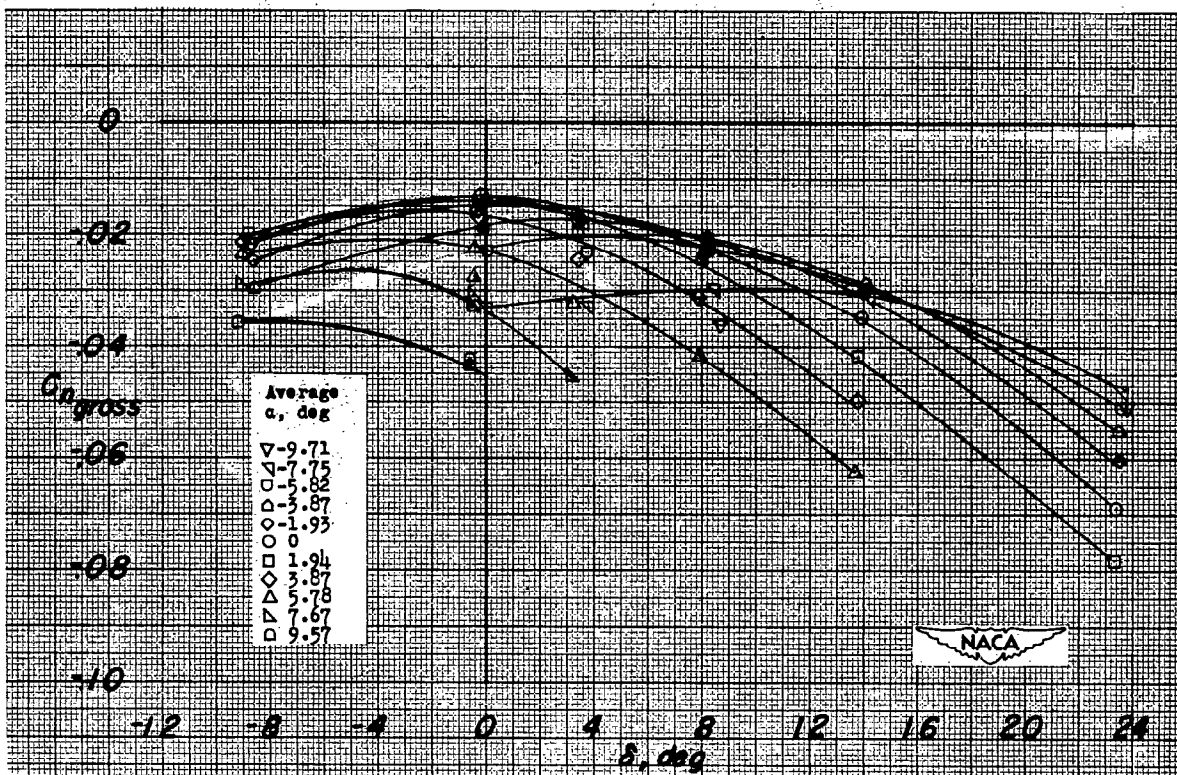
(c) Elevator hinge moment.

Figure 7.- Continued.



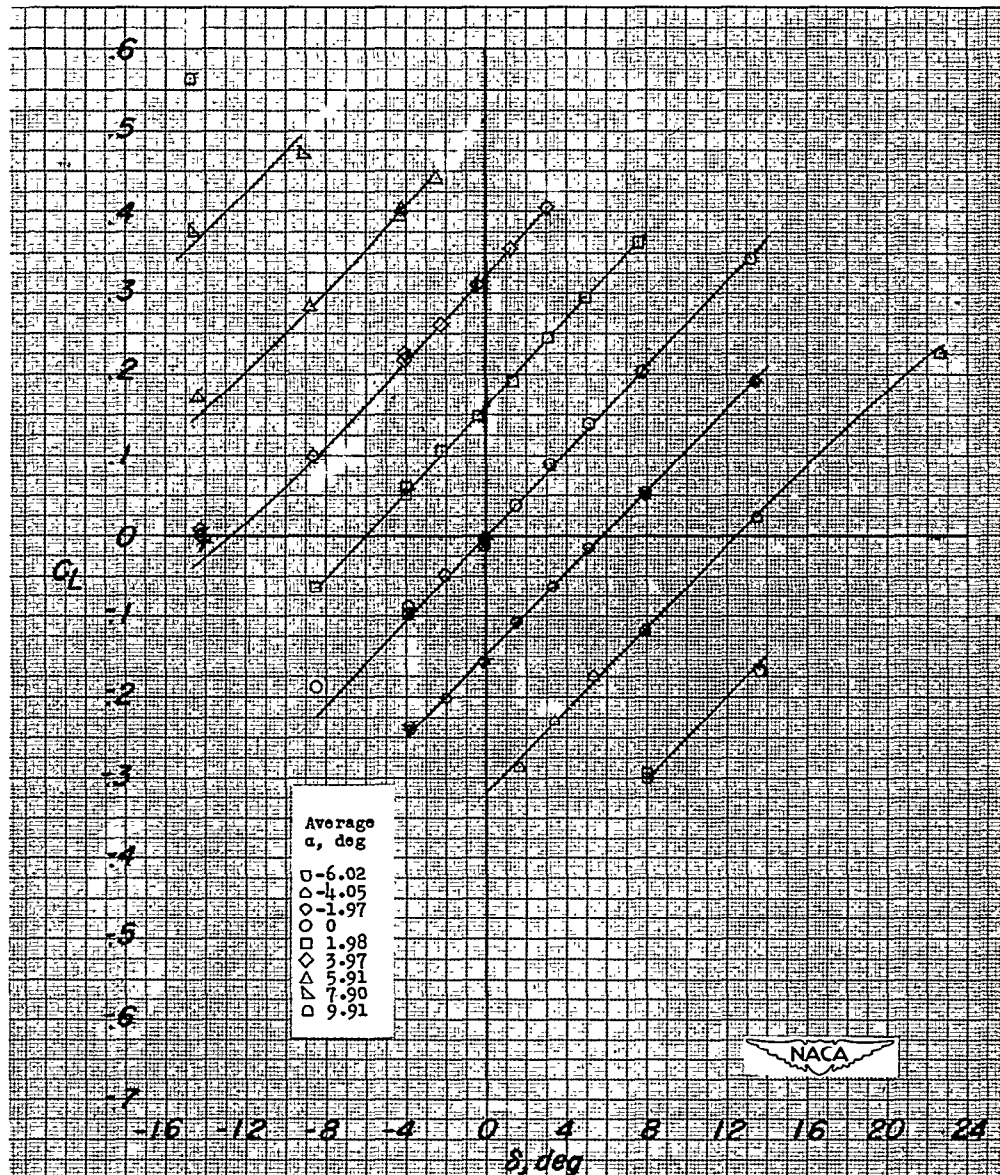
(e) Rolling moment.

Figure 7.- Continued.



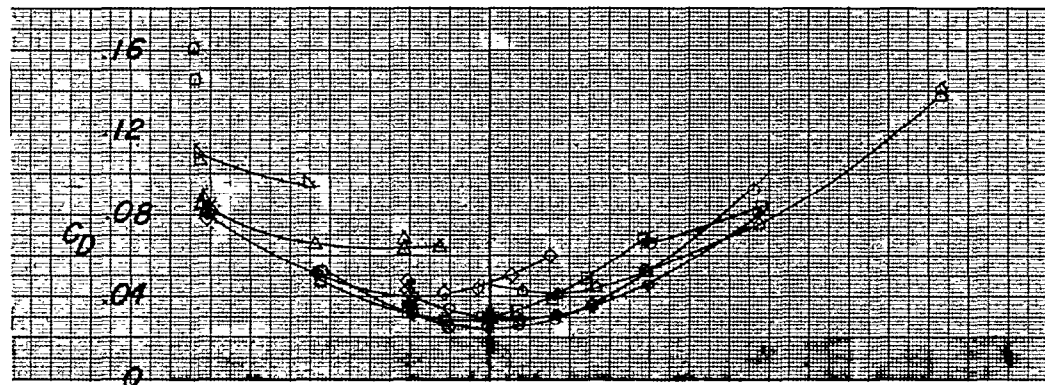
(f) Yawing moment.

Figure 7.- Concluded.

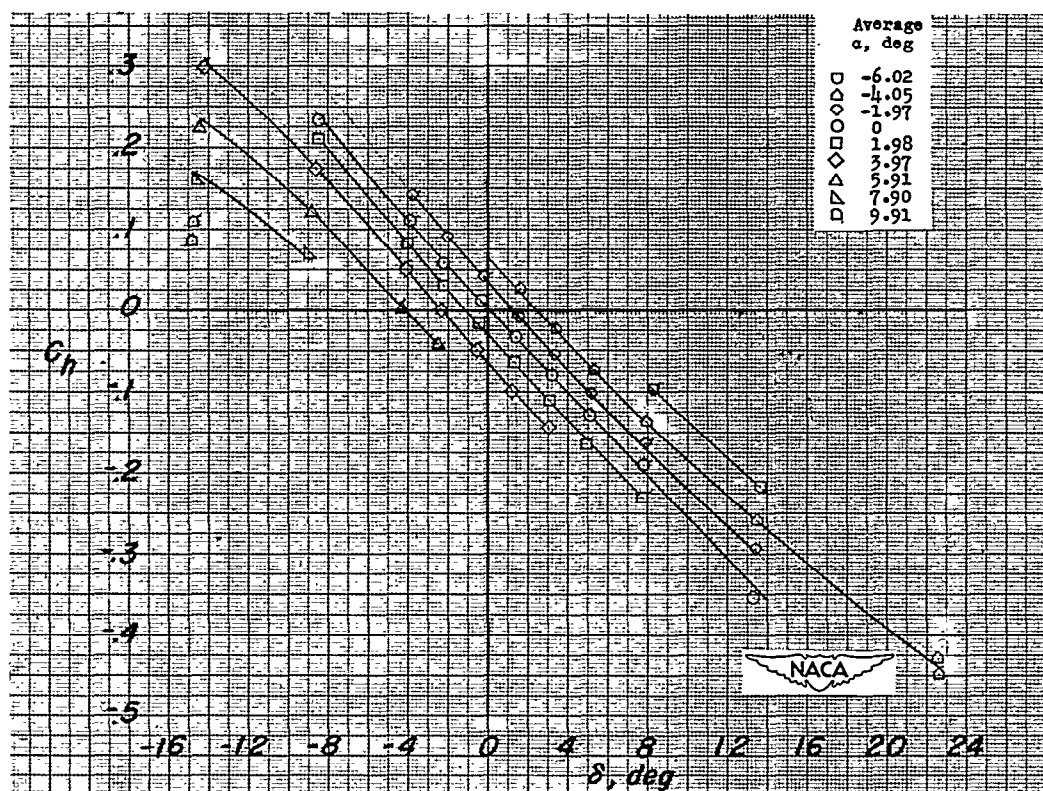


(a) Lift.

Figure 8.- Variation of aerodynamic characteristics with elevator deflection of 0.6-scale model of Falcon (MX-904) tail surface in the presence of half-span body (B_3T); $M = 1.62$. (Flagged symbols denote check tests.)

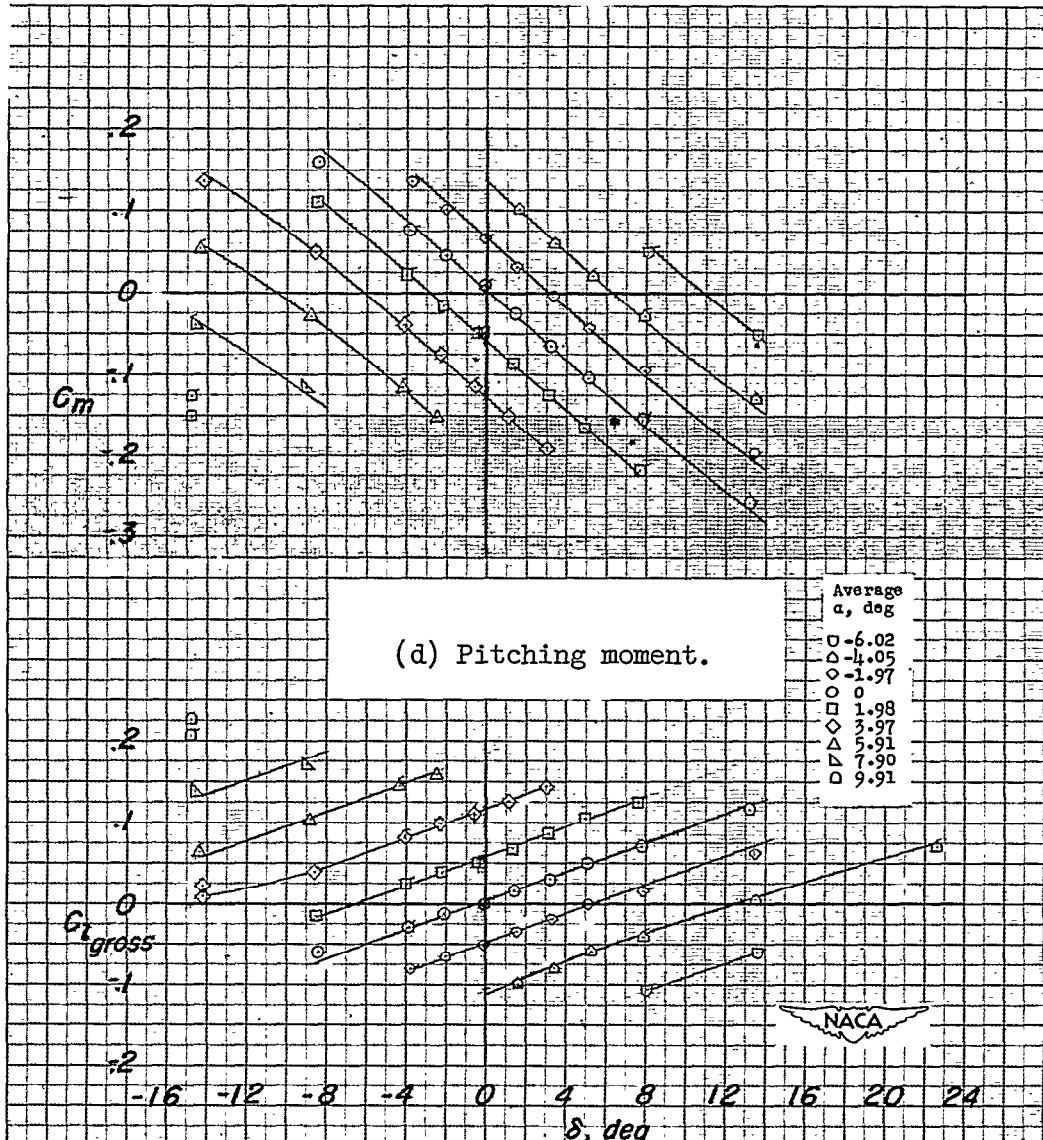
P.
C.
O.
R.

(b) Drag.



(c) Elevator hinge moment.

Figure 8.- Continued.



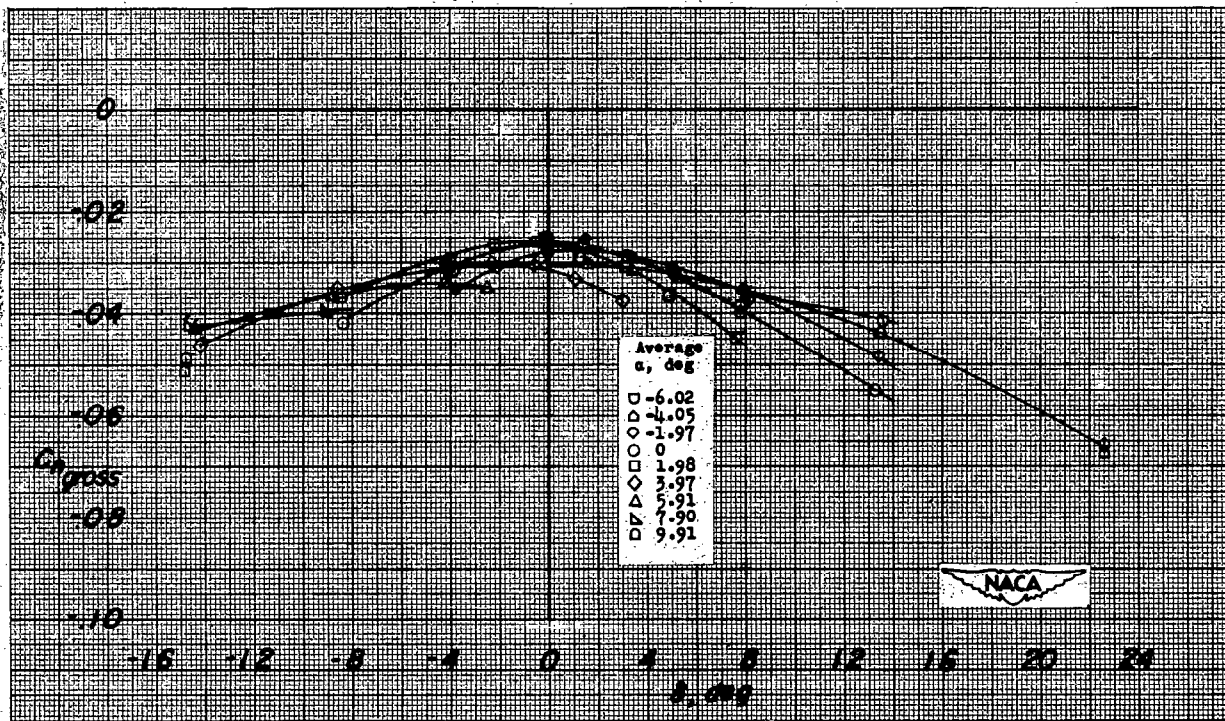
(e) Rolling moment.

Figure 8.- Continued.

32178

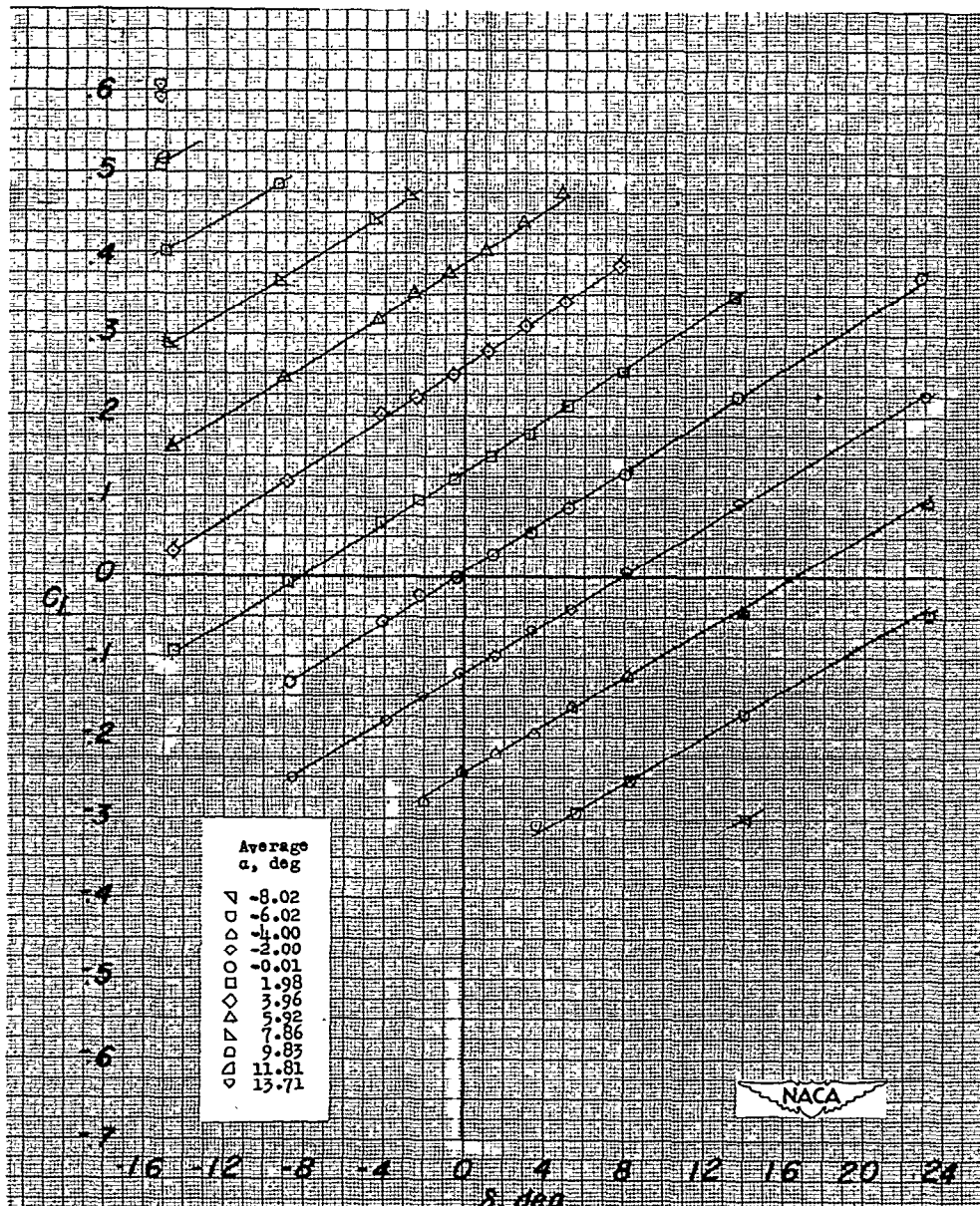
NACA RM SL50G13

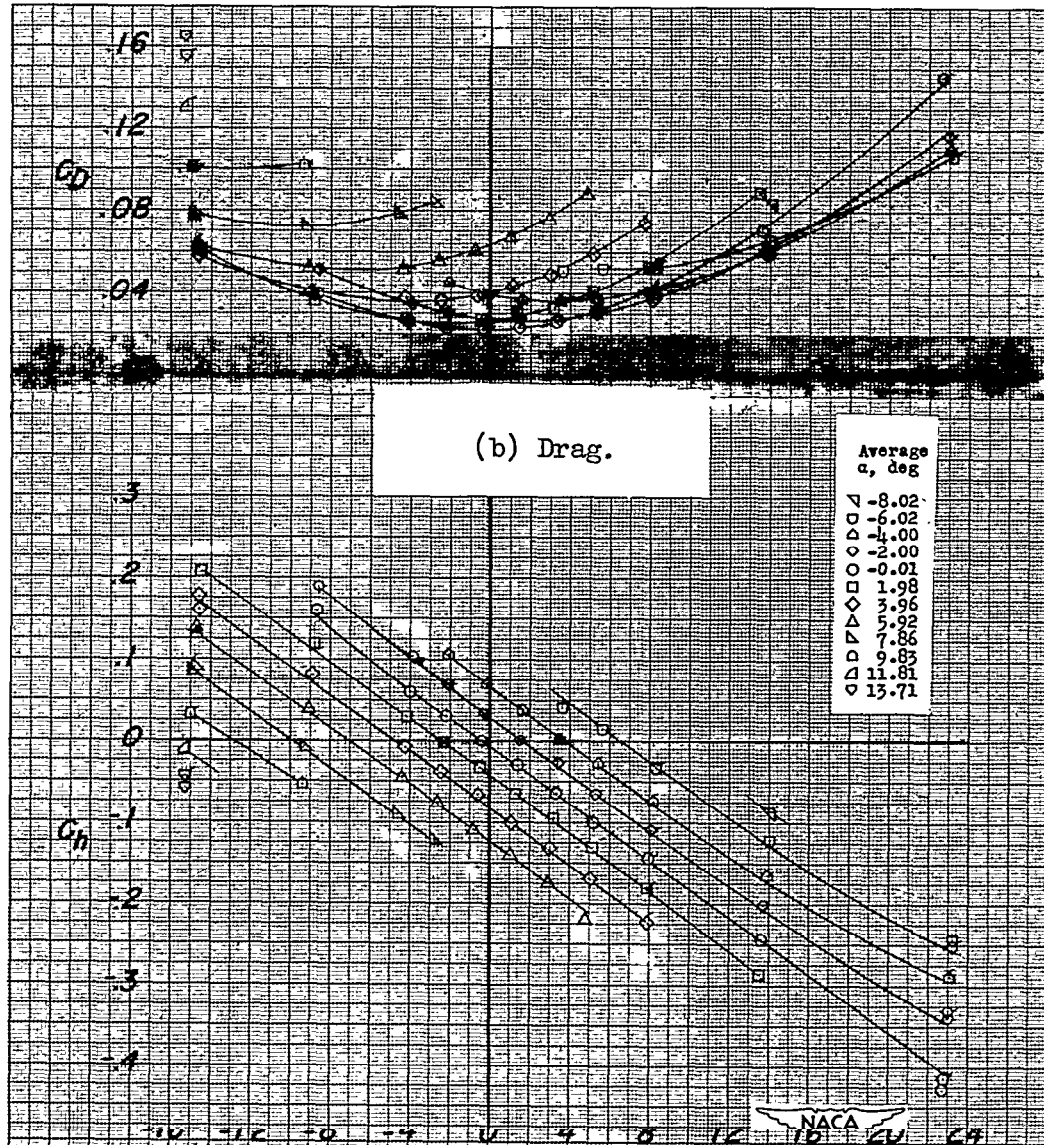
CONTINUED

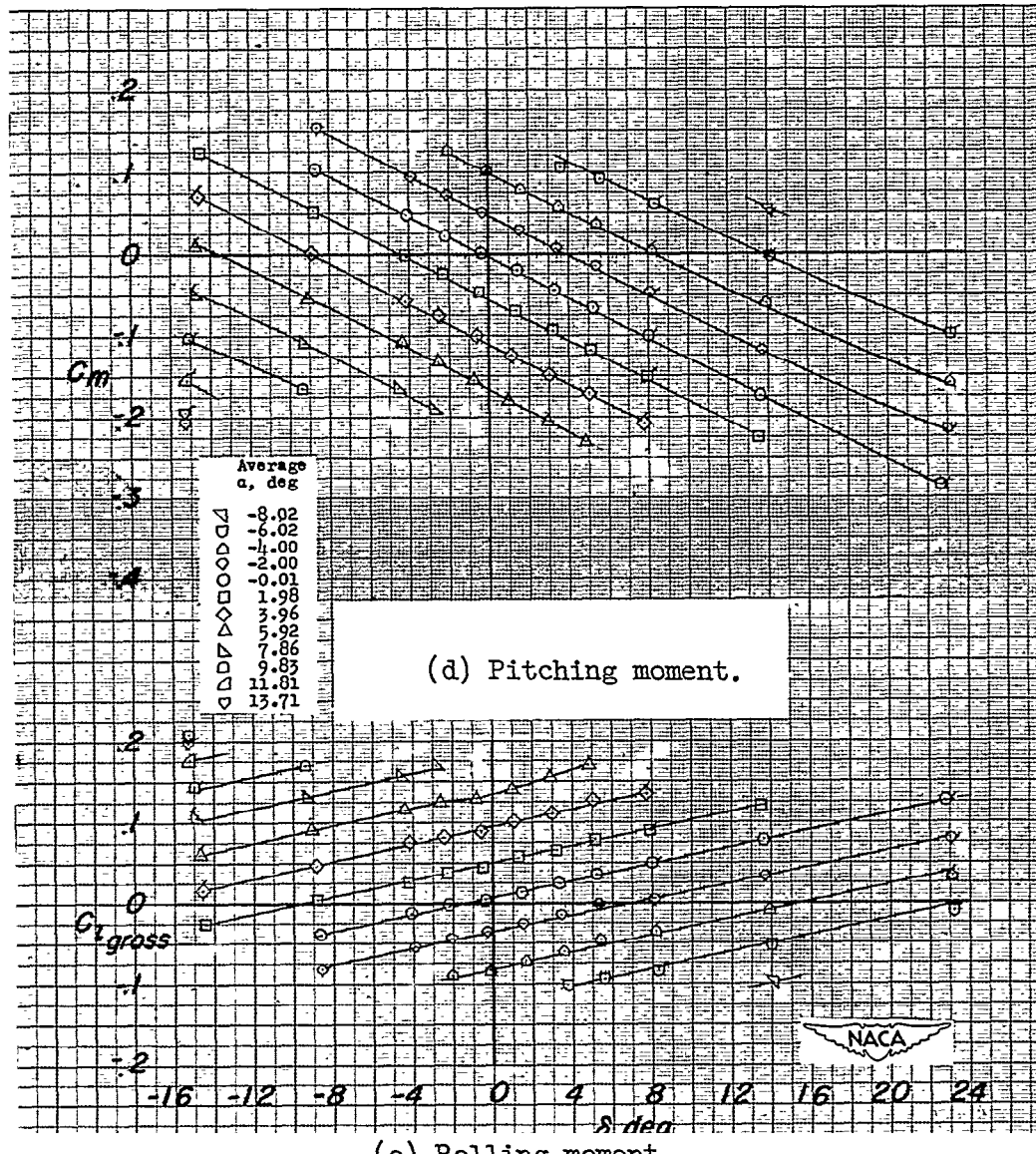


(f) Yawing moment.

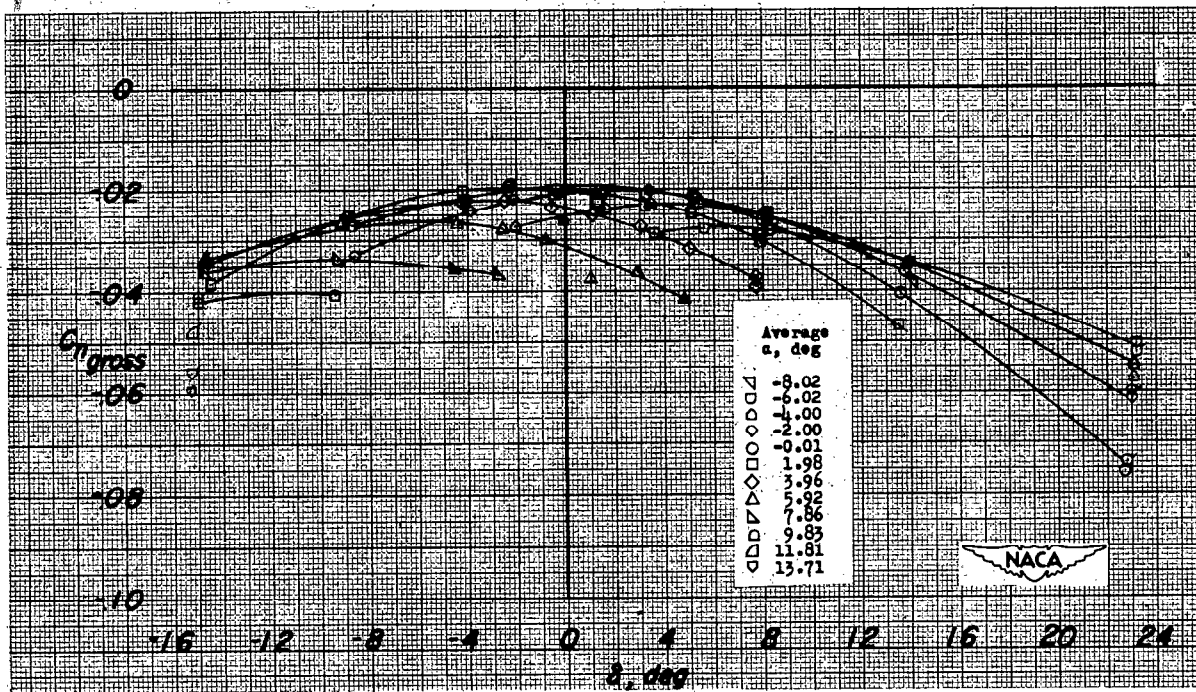
Figure 8.- Concluded.



R
M
C
P

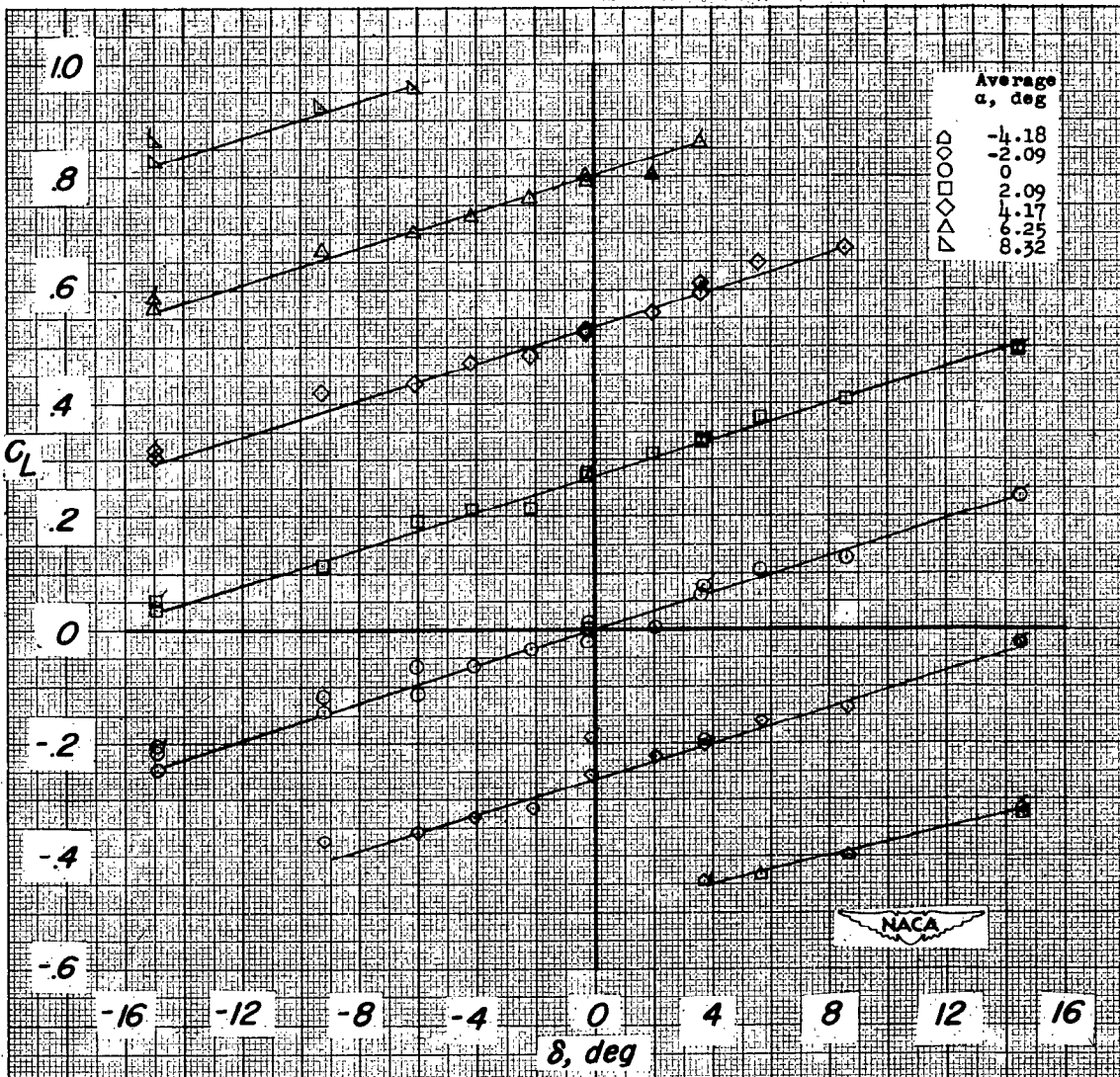


32179



(f) Yawing moment.

Figure 9.- Concluded.

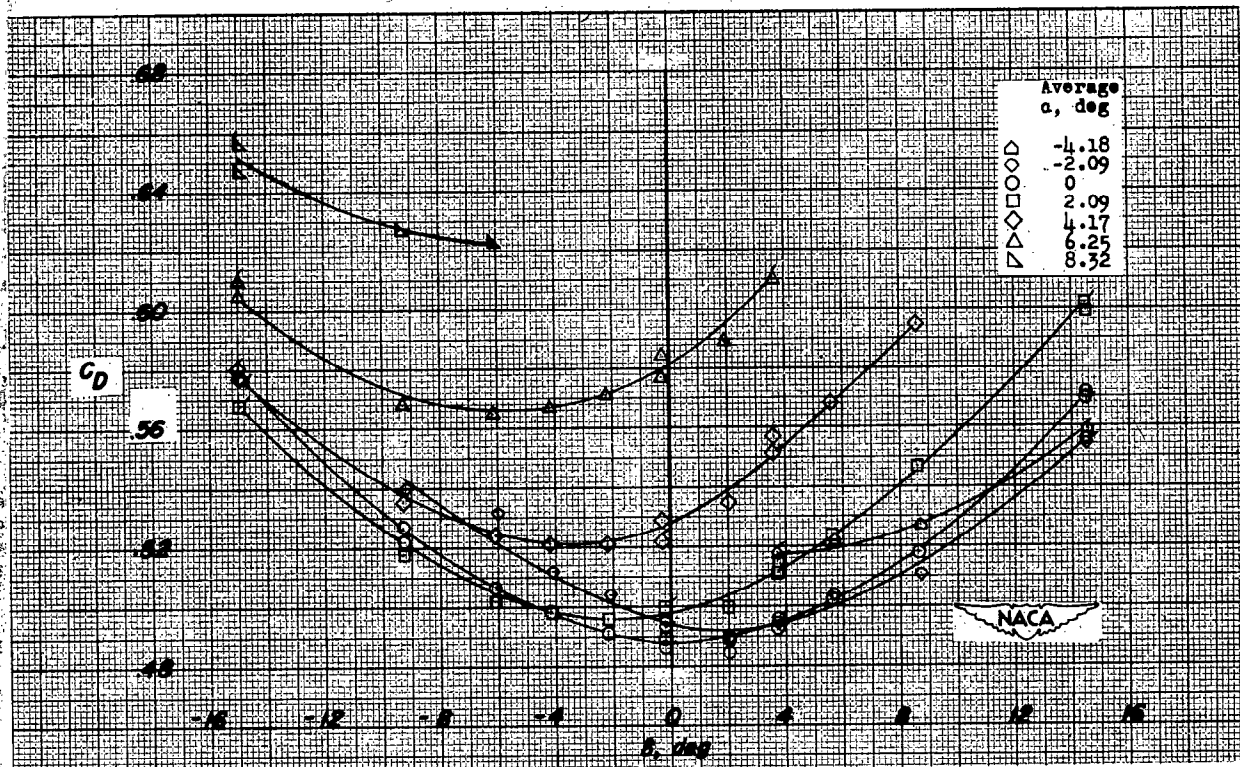


(a) Lift.

Figure 10.- Variation of aerodynamic characteristics with elevator deflection of 0.6-scale model of Falcon (MX-904) tail surface attached to half-span body (BHT); $M = 1.96$. (Flagged symbols denote check tests.)

331710

NACA RM SL50G13

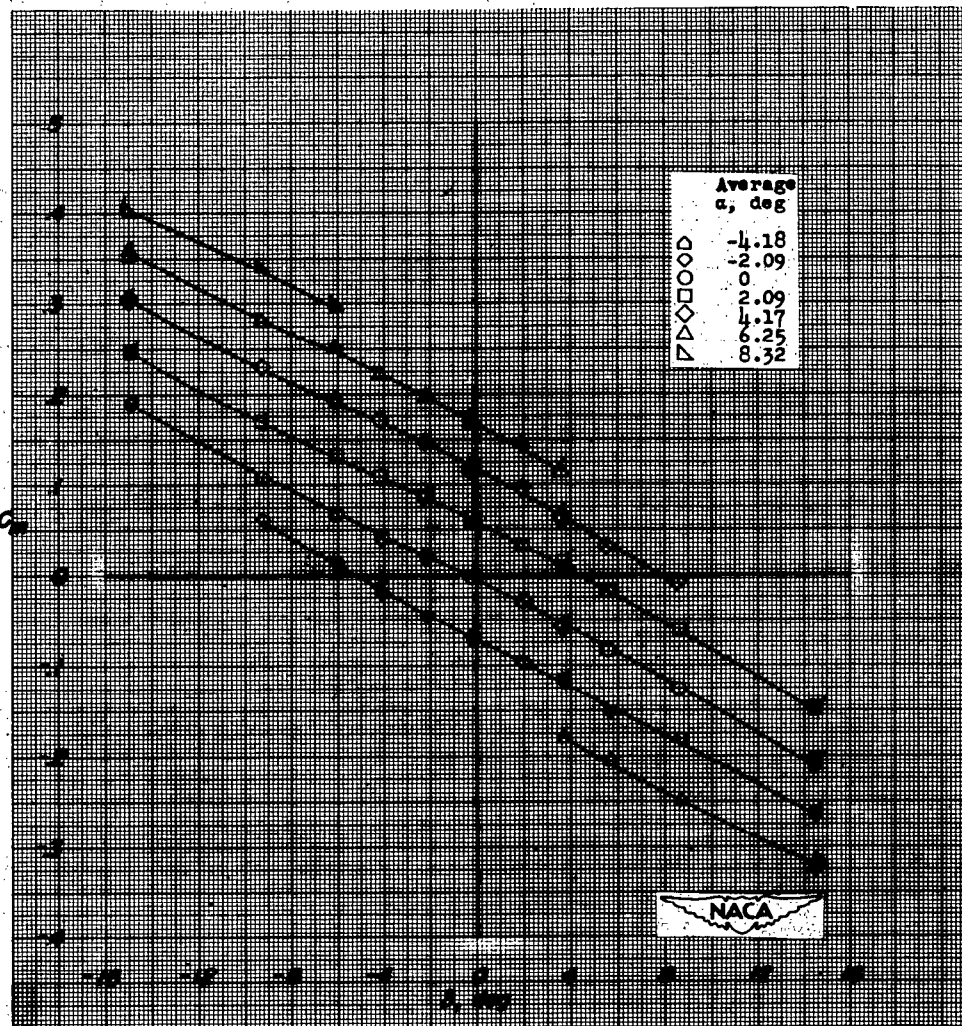


(b) Drag.

Figure 10.- Continued.

NACA RM SL50G13

~~CONFIDENTIAL~~



(c) Pitching moment.

Figure 10.- Continued.

~~CONFIDENTIAL~~

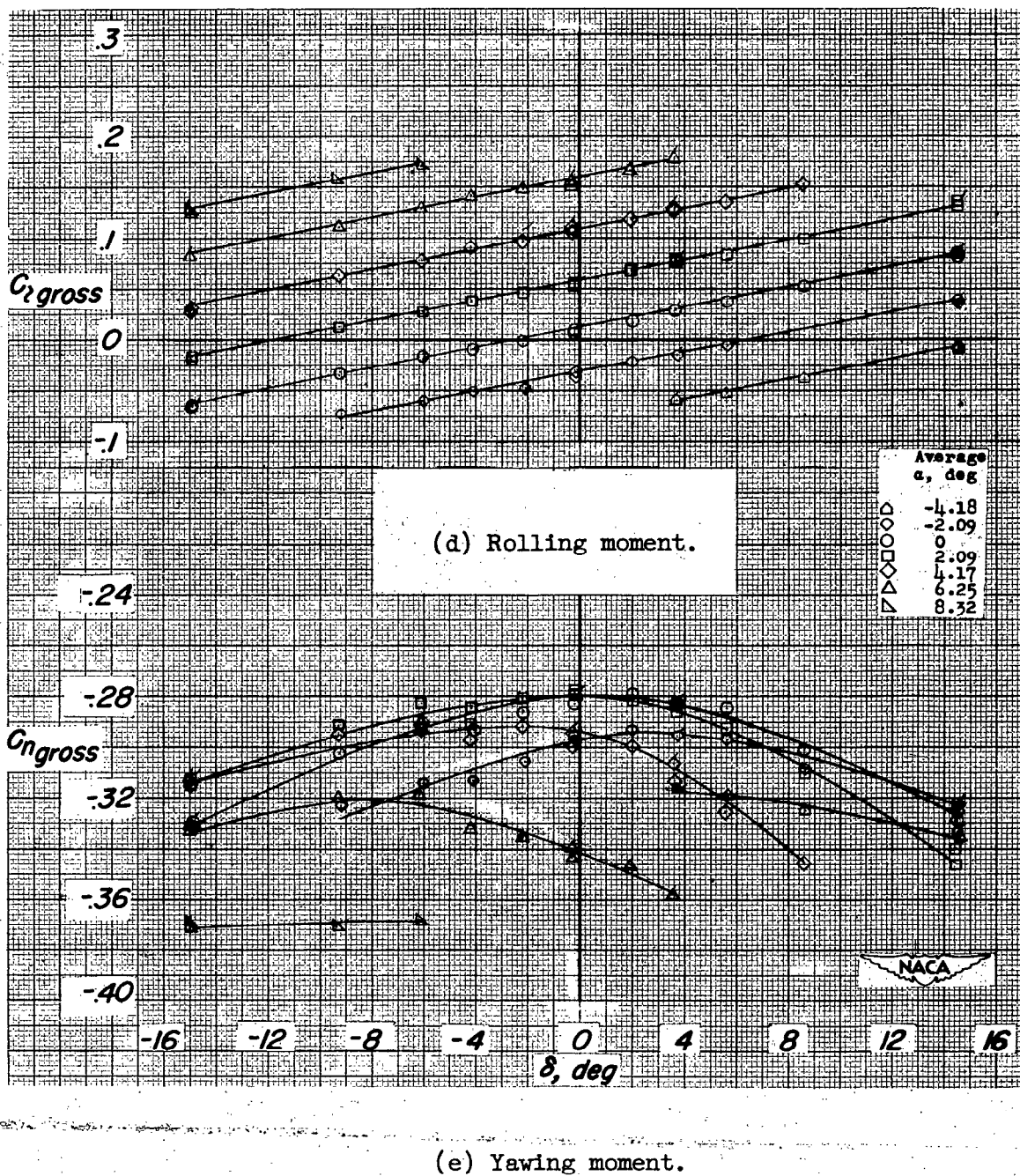
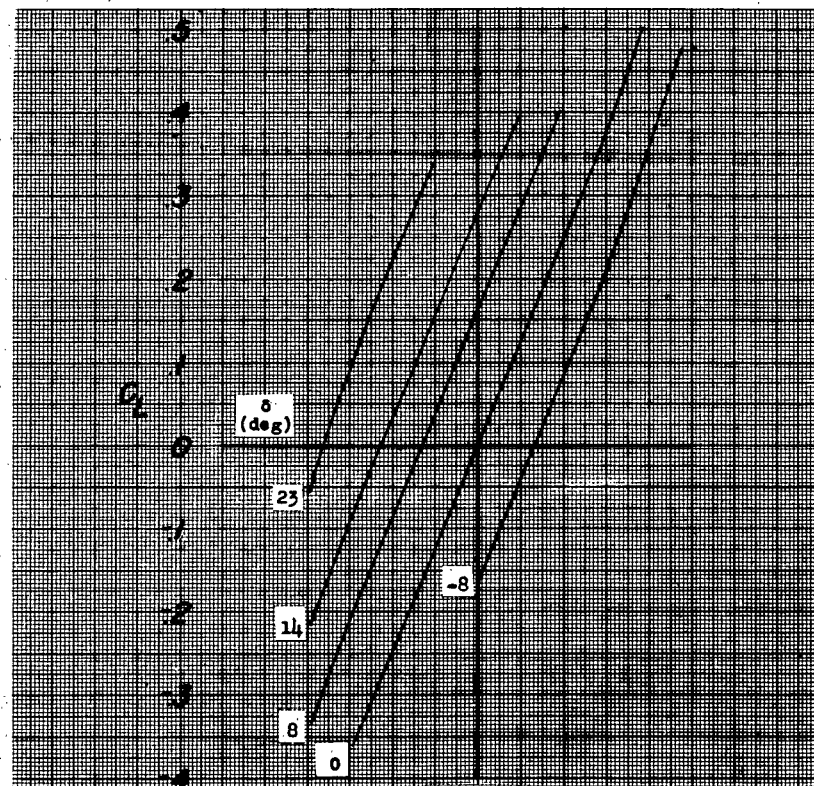
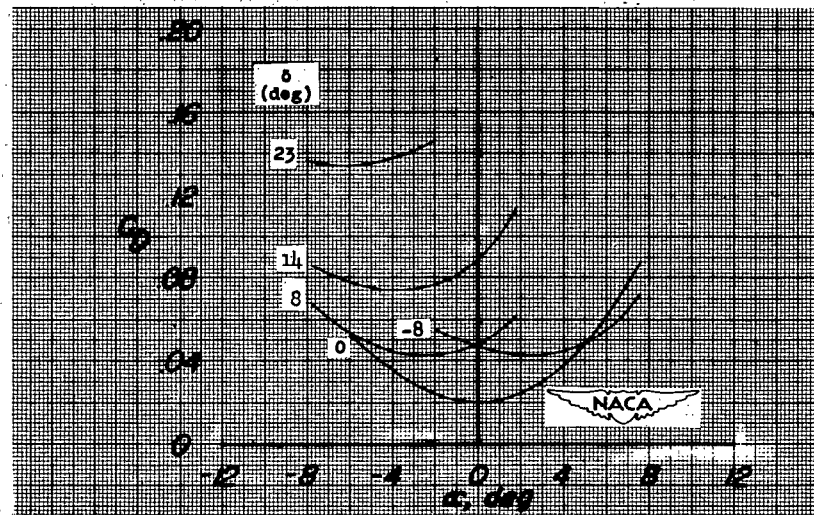


Figure 10.- Concluded.

NACA RM SL50G13



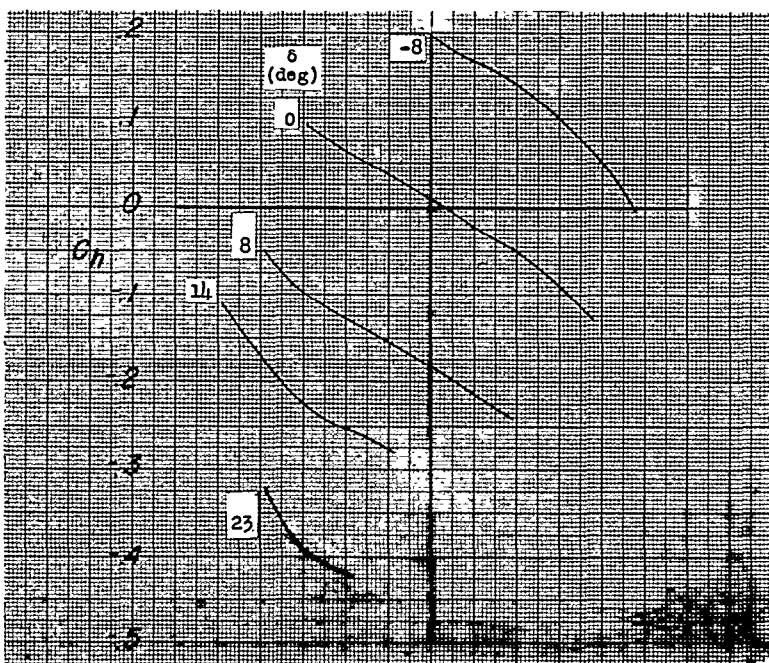
(a) Lift.



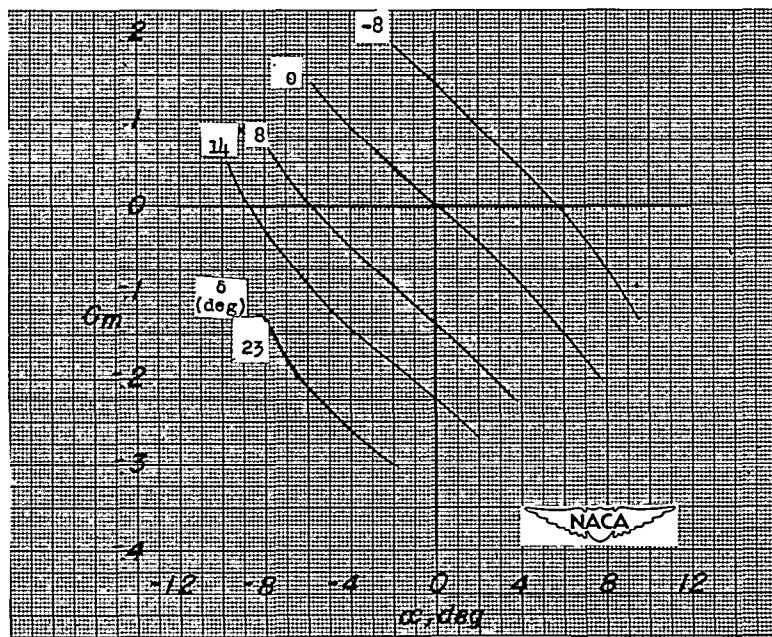
(b) Drag.

Figure 11.- Variation of aerodynamic characteristics with angle of attack of 0.6-scale model of Falcon (MX-904) tail surface in the presence of partial-span body (B_1T); $M = 1.62$.

~~CONFIDENTIAL~~

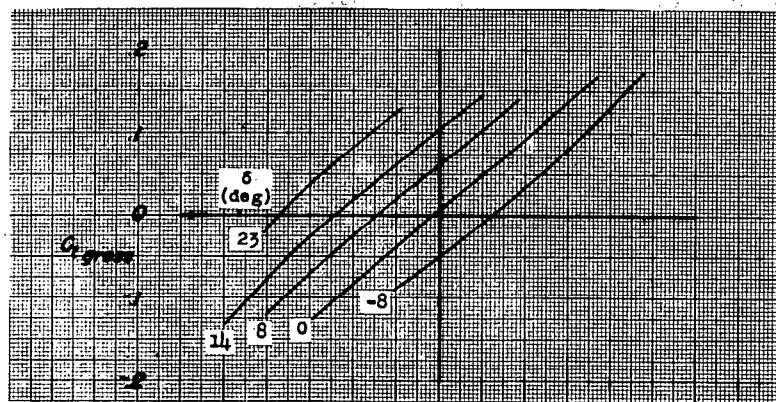


(c) Elevator hinge moment.

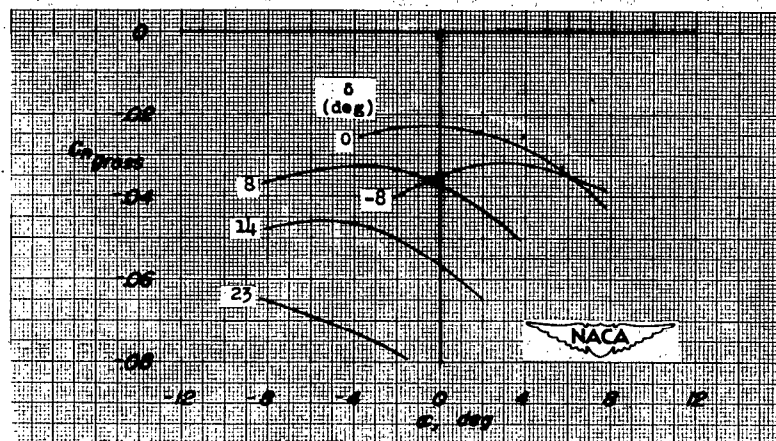


(d) Pitching moment.

Figure 11.- Continued.



(e) Rolling moment.

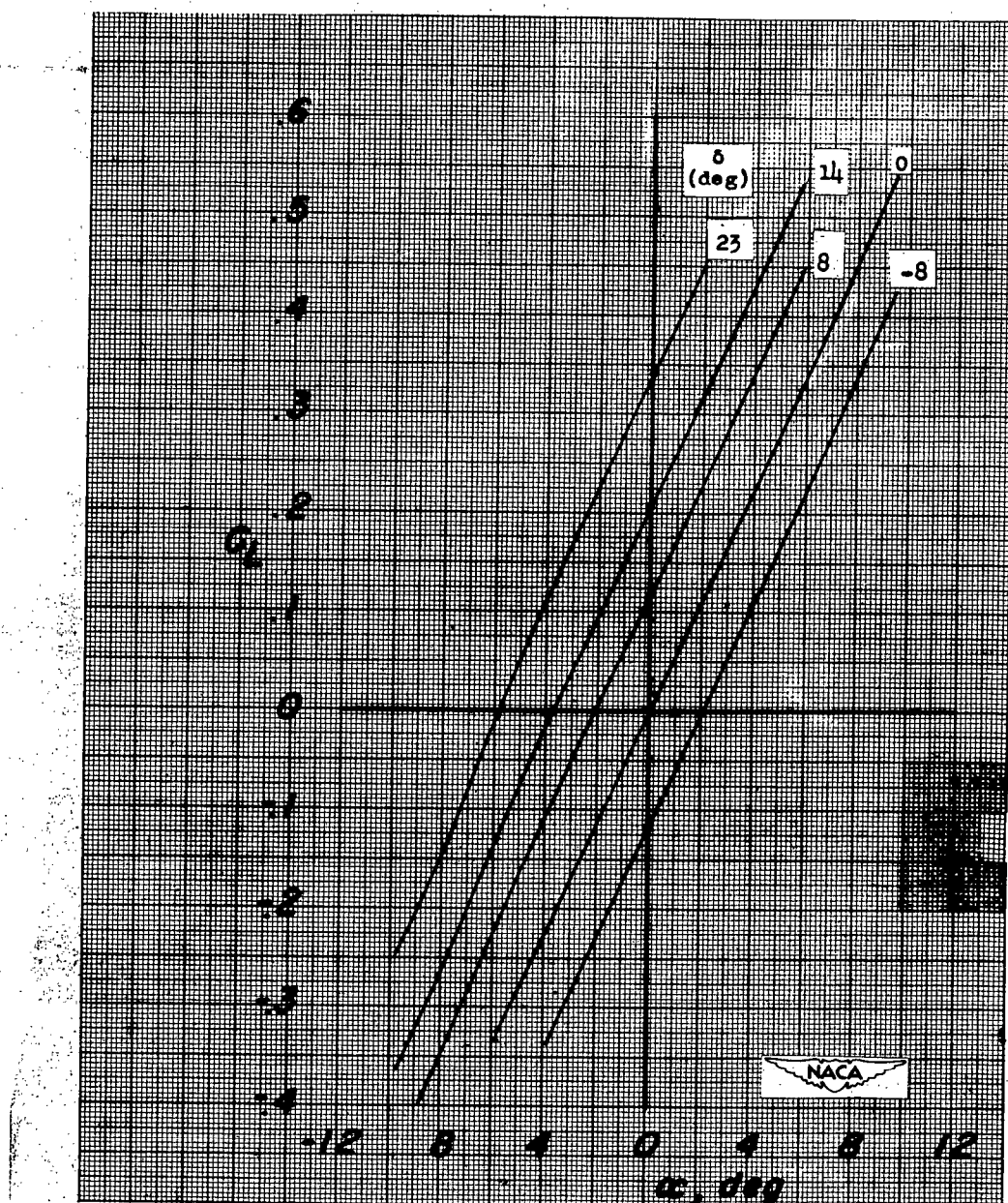


(f) Yawing moment.

Figure 11.- Concluded.

NACA RM SL50G13

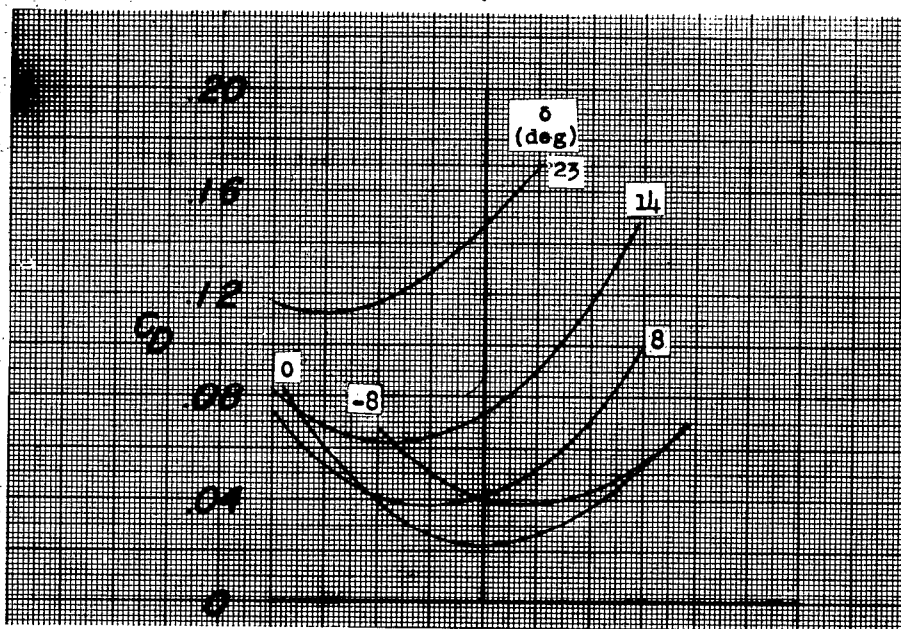
~~CONFIDENTIAL~~



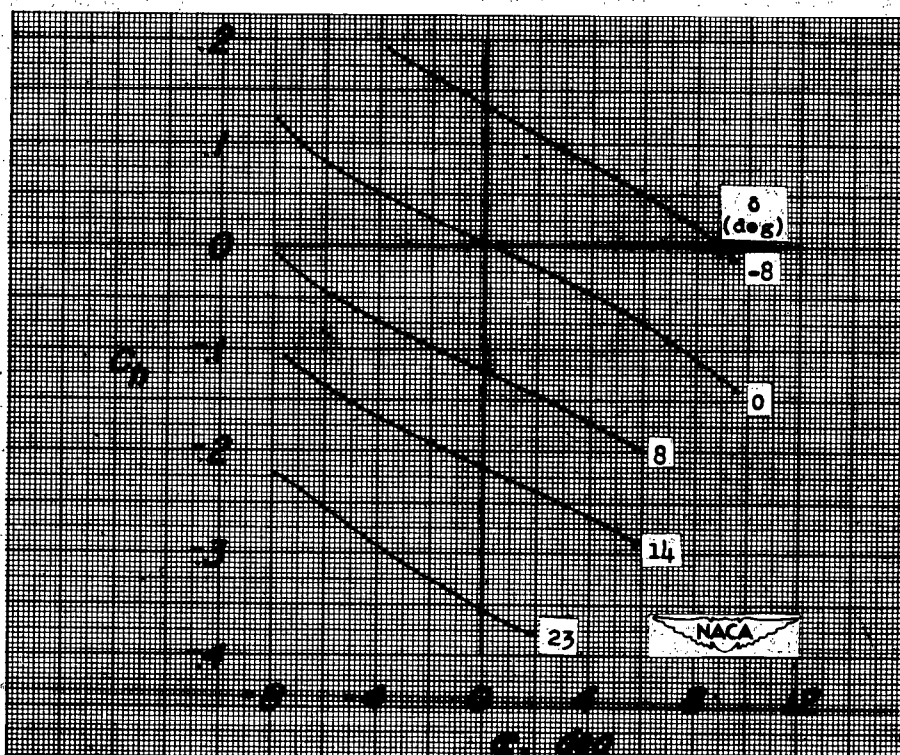
(a) Lift.

Figure 12.- Variation of aerodynamic characteristics with angle of attack of 0.6-scale model of Falcon (MX-904) tail surface in the presence of partial-span body (B_1T); $M = 1.96$.

~~CONFIDENTIAL~~

~~CONFIDENTIAL~~

(b) Drag.



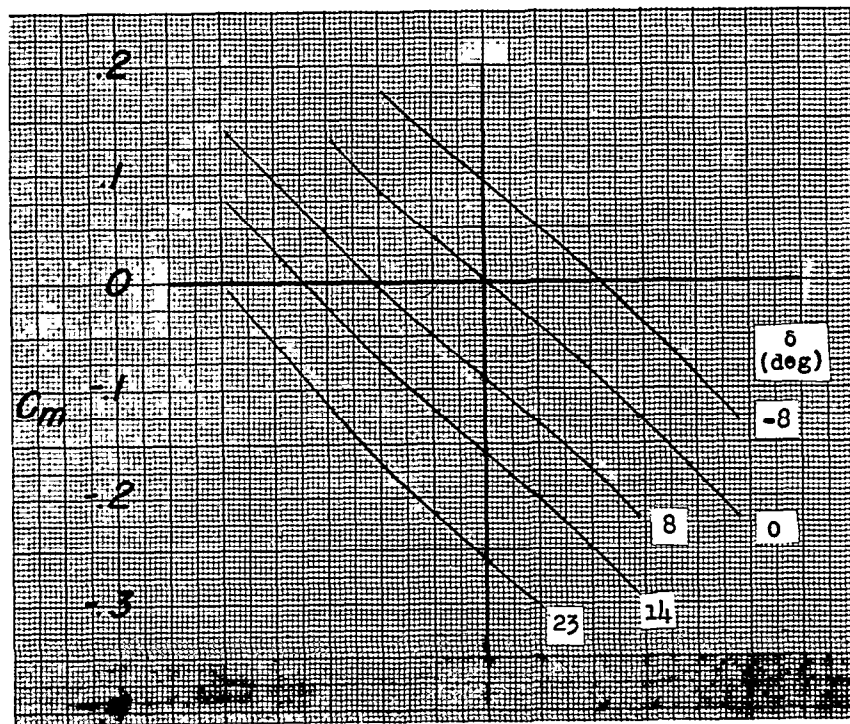
(c) Elevator hinge moment.

Figure 12.- Continued.

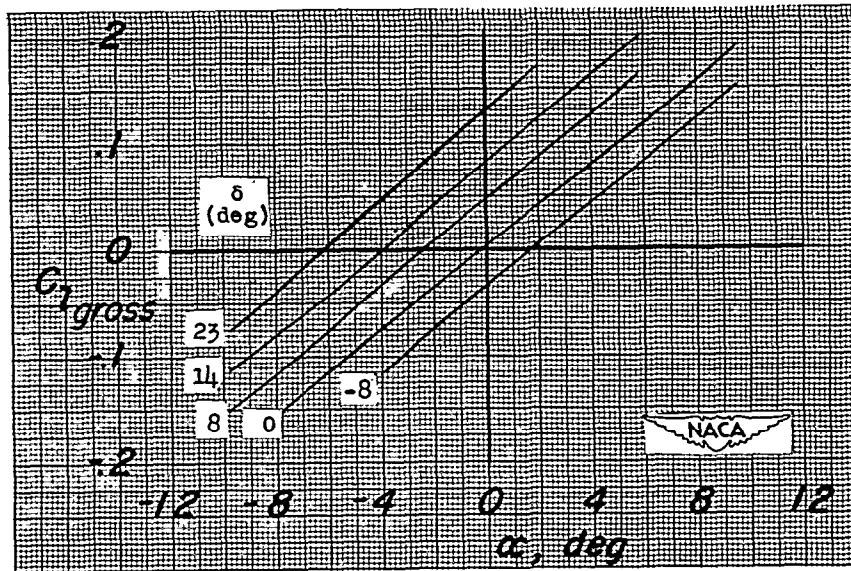
~~CONFIDENTIAL~~

9
10
11
12
13
14

NACA RM SL50G13



(d) Pitching moment.



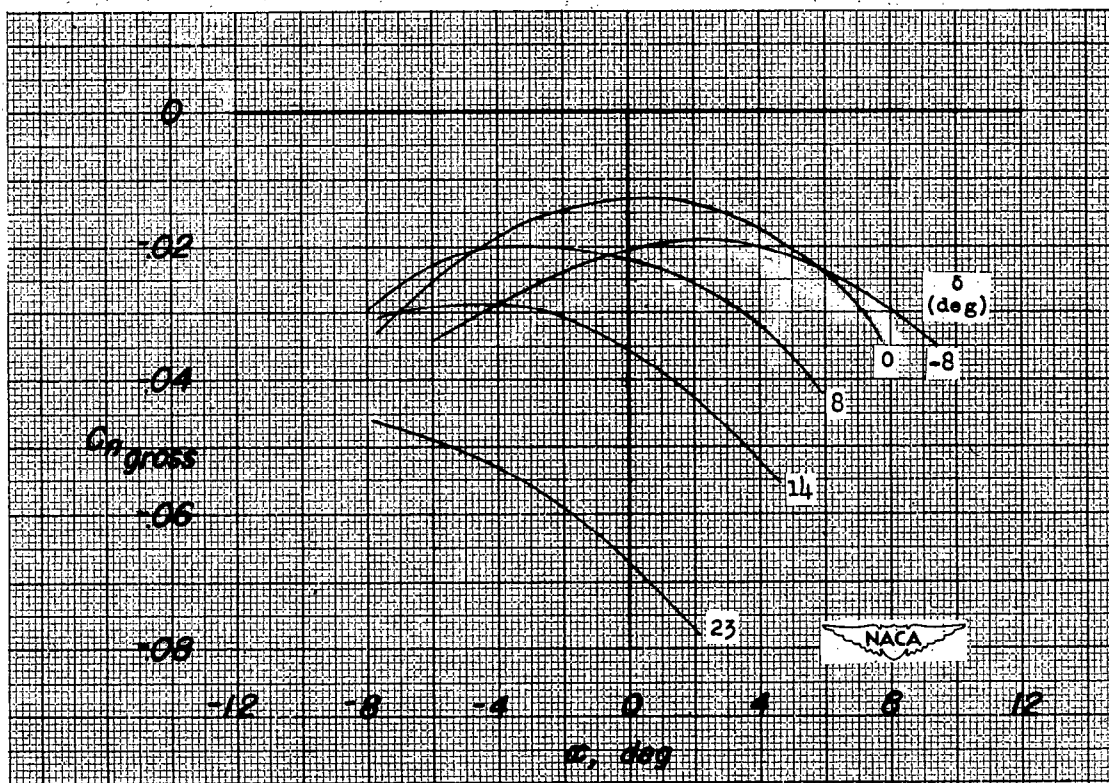
(e) Rolling moment.

Figure 12.- Continued.

321712

NACA RM SL50G13

CONFIDENTIAL

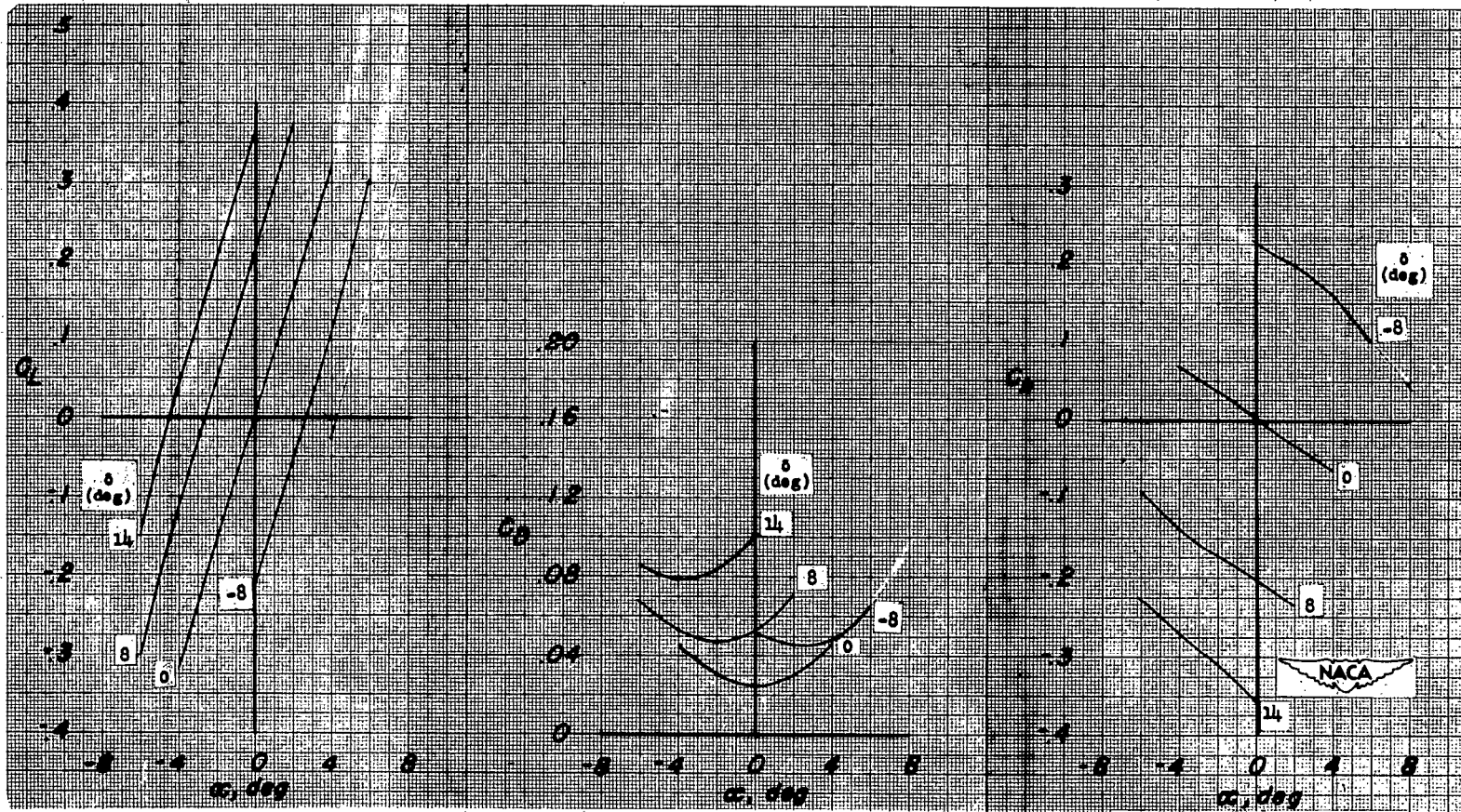


(f) Yawing moment.

Figure 12.- Concluded.

321713

NACA RM SL50C13



(a) Lift.

(b) Drag.

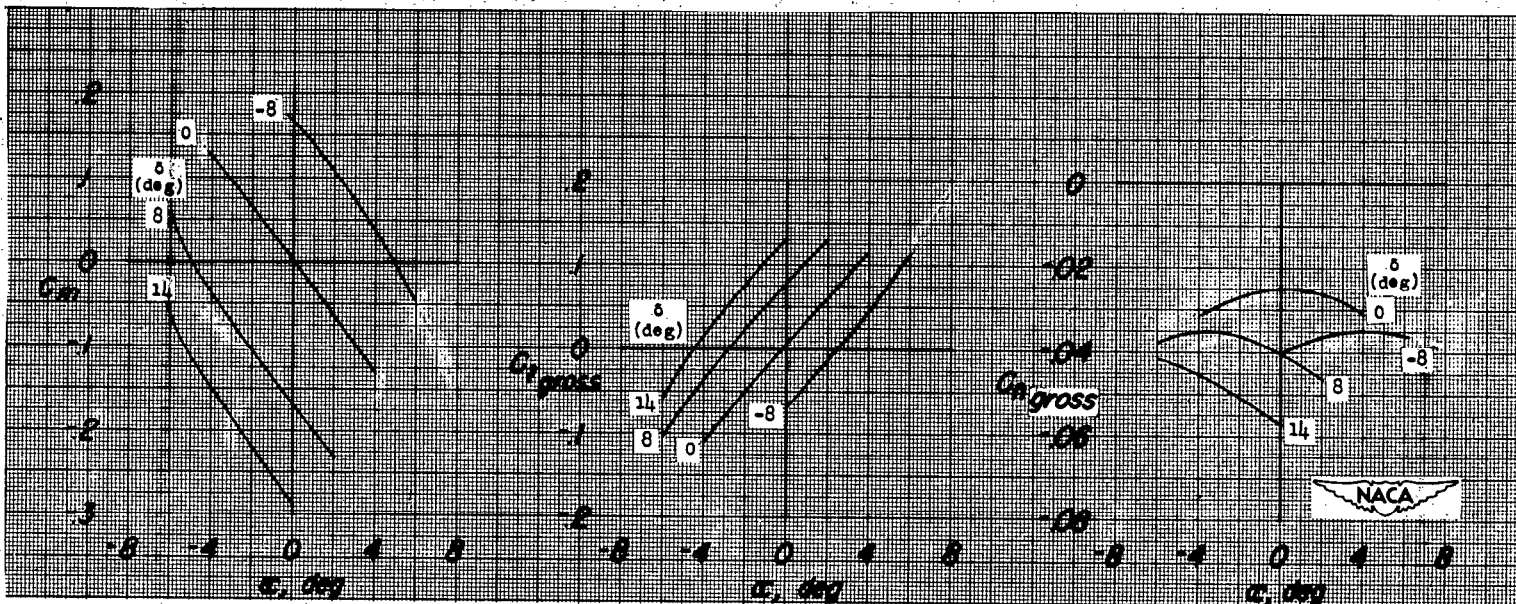
(c) Elevator hinge moment.

Figure 13.- Variation of aerodynamic characteristics with angle of attack of 0.6-scale model of Falcon (MX-904) tail surface in the presence of half-span body (B_3T); $M = 1.62$.

321713

NACA RM SL50013

CONFIDENTIAL



(d) Pitching moment. (e) Rolling moment. (f) Yawing moment.

Figure 13.- Concluded.

321734

NACA RM SL50G13

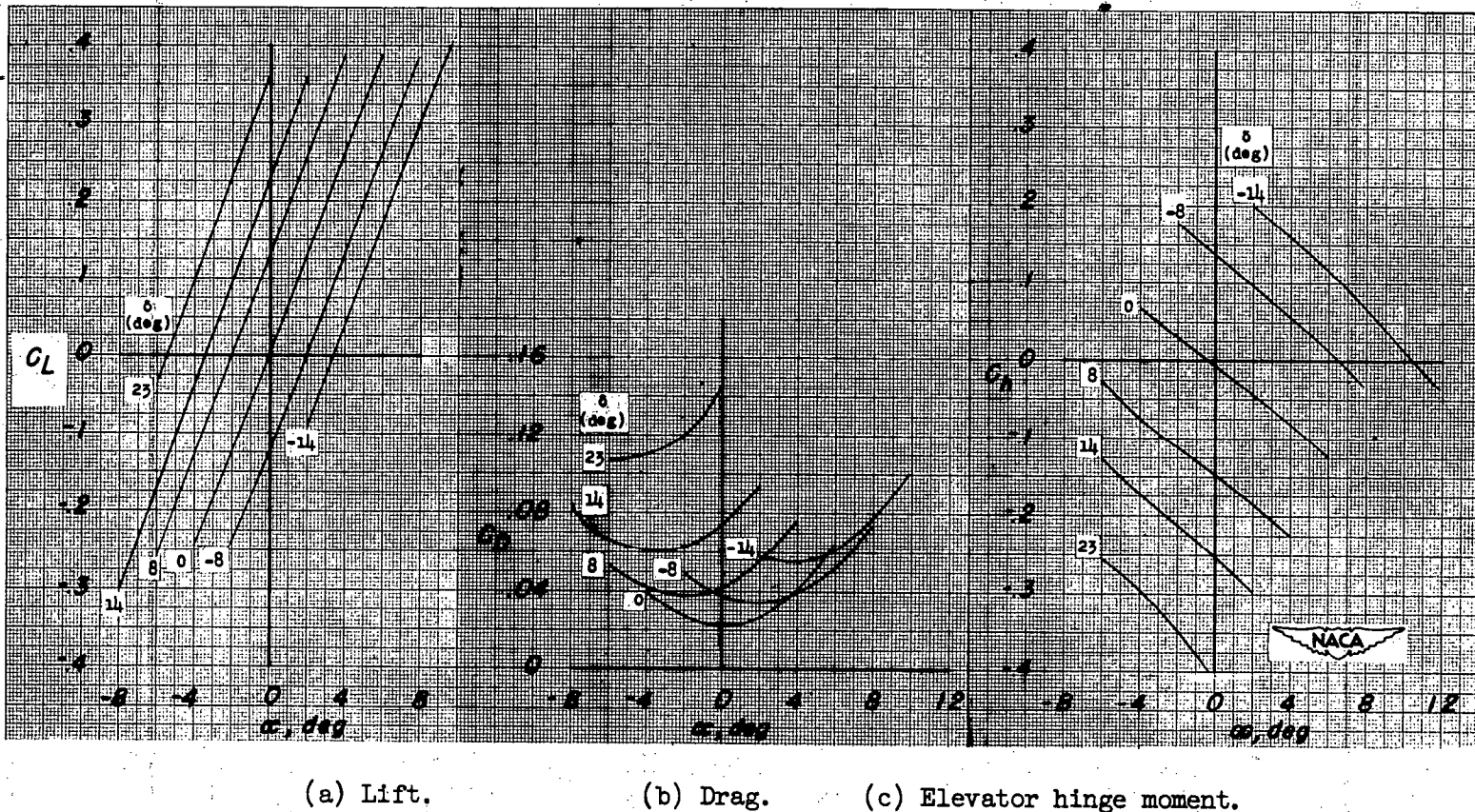
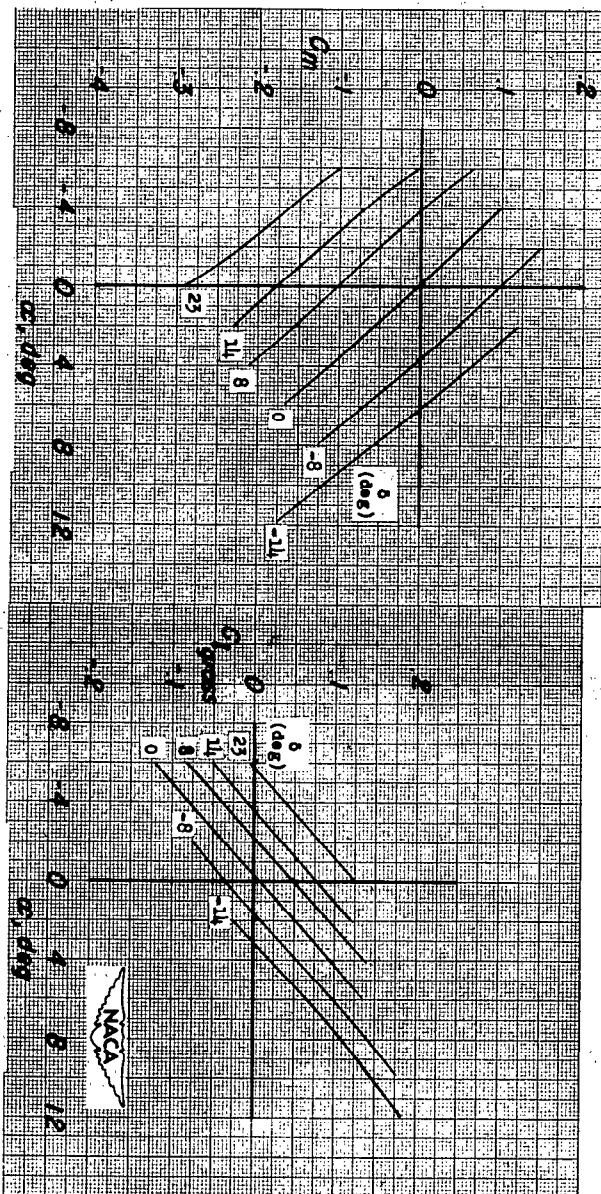
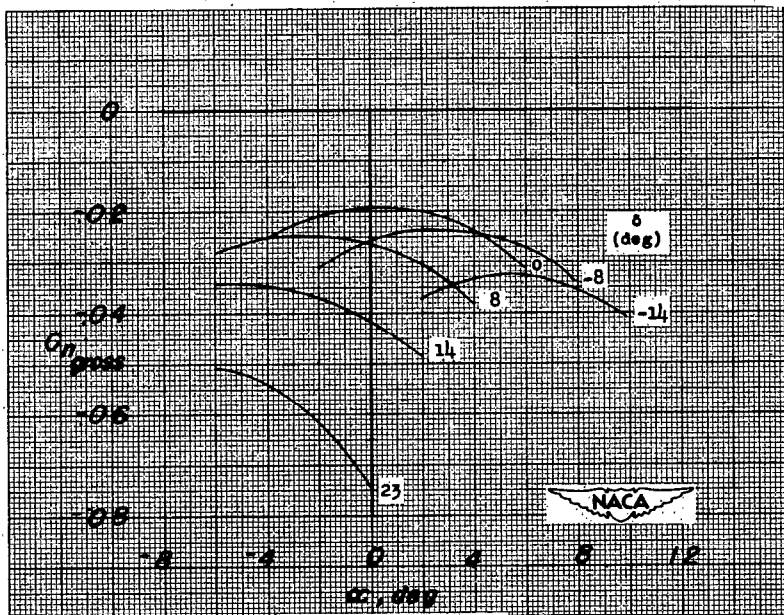


Figure 14.- Variation of aerodynamic characteristics with angle of attack of 0.6-scale model of Falcon (MX-904) tail surface in the presence of half-span body (B₃T); M = 1.96.



(d) Pitching moment. (e) Rolling moment.

Figure 14.- Continued.

~~CONFIDENTIAL~~

(f) Yawing moment.

Figure 14.- Concluded.

~~CONFIDENTIAL~~

381746

NACA RM SL50G13

CONFIDENTIAL

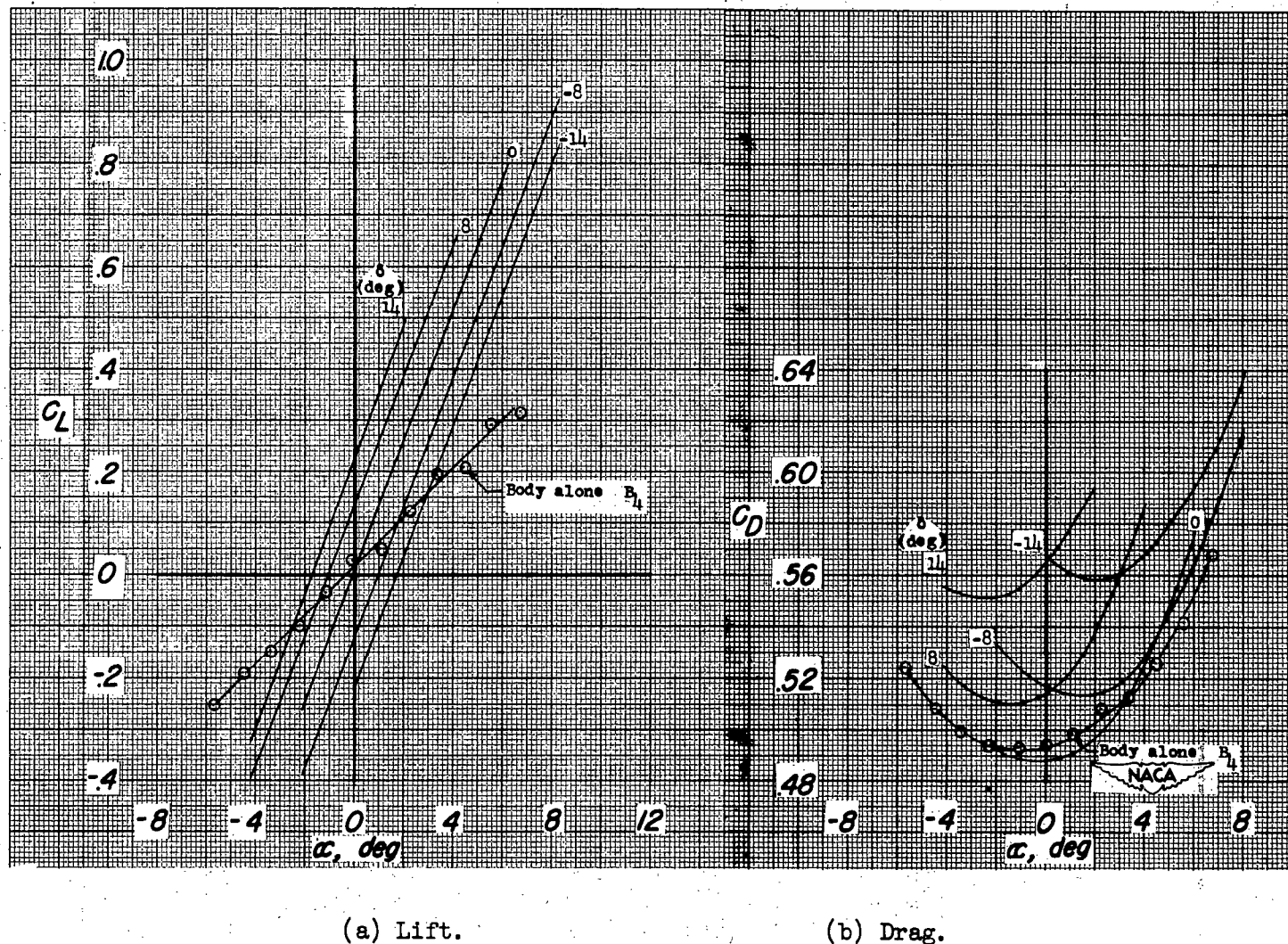
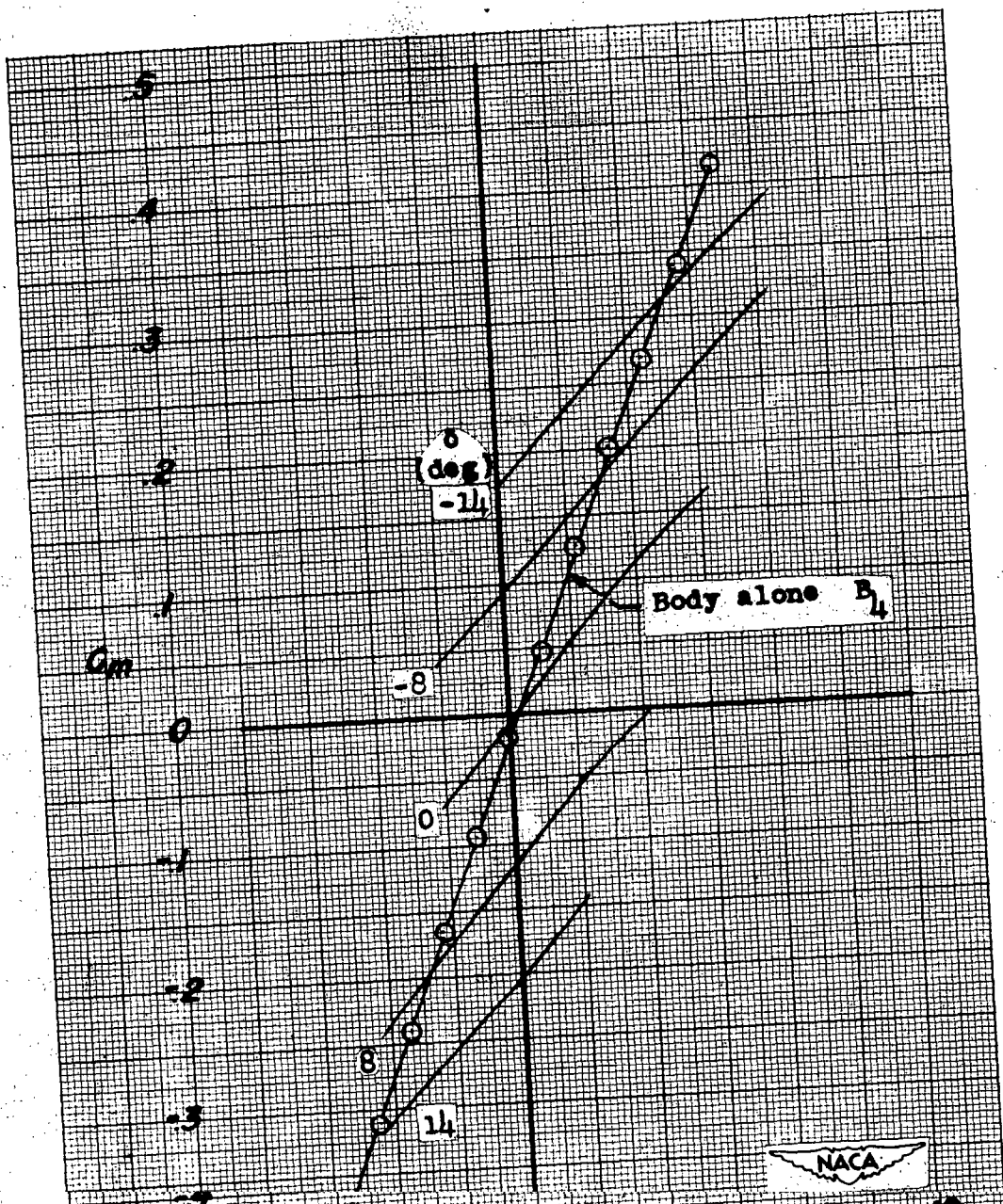


Figure 15.- Variation of aerodynamic characteristics with angle of attack of 0.6-scale model of Falcon (MX-904) tail surface attached to half-span body (B_4T); $M = 1.96$.

NACA RM SL50G13

~~CONFIDENTIAL~~



NACA

324716

NACA RM SL50G13

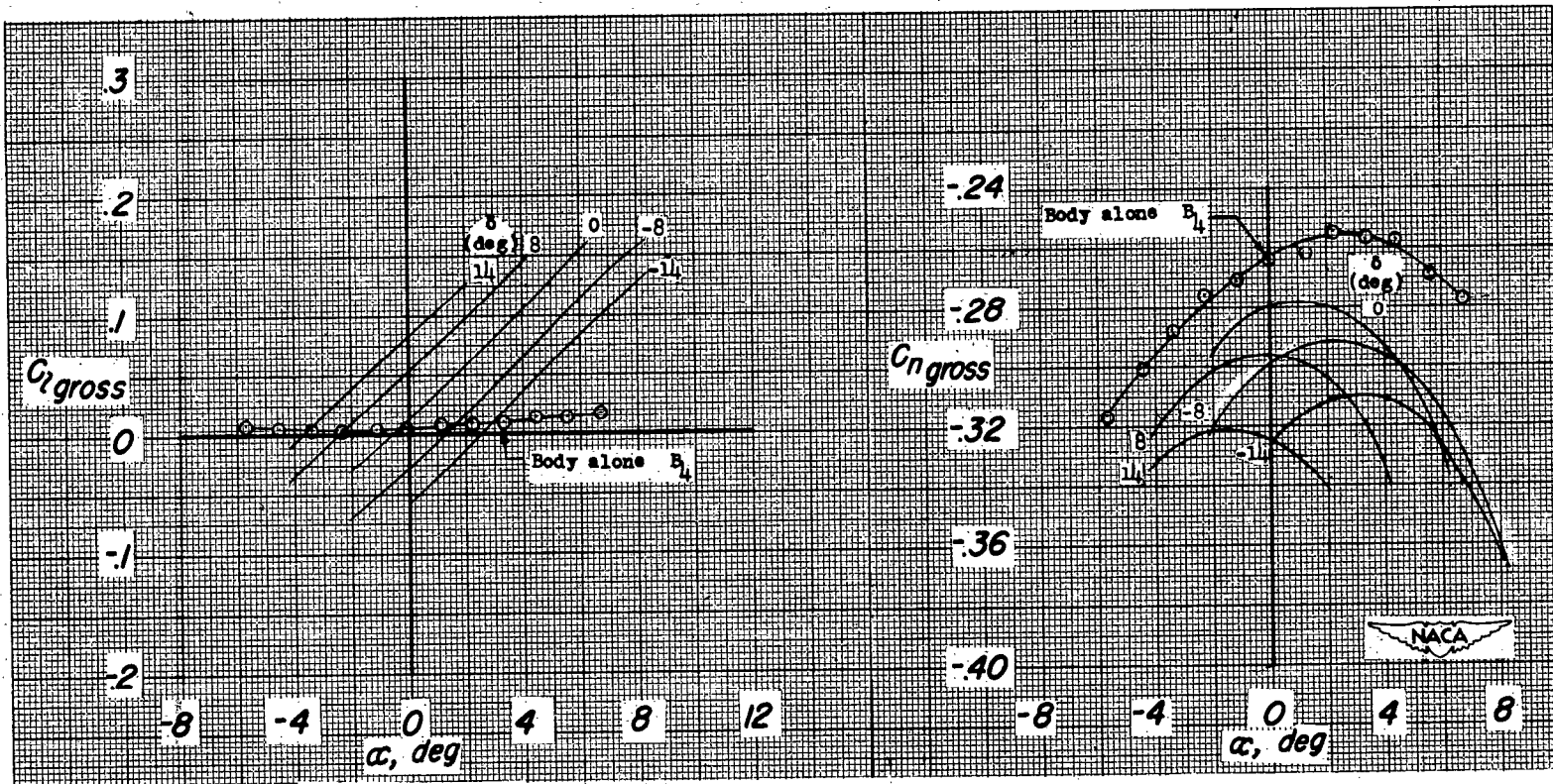


Figure 15.- Concluded.

NACA RM SL50G13

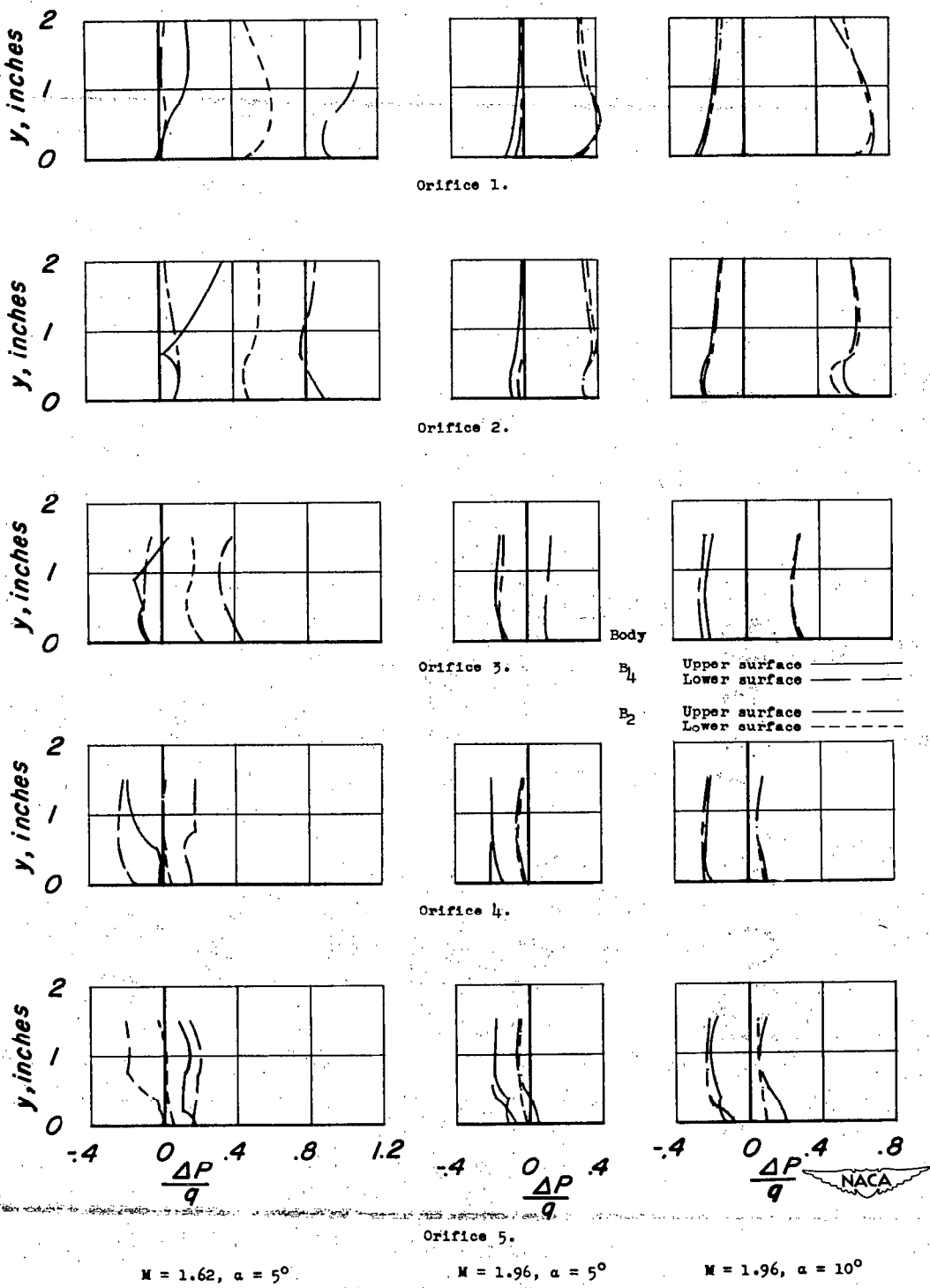


Figure 16.- Pressure measurements obtained on a two-dimensional unswept airfoil near the juncture with semispan body B_4 and partial-span body B_2 .

3 1176 01438 5489



NASA Technical Library

